CHALMERS
UNIVERSITY OF TECHNOLOGY

Modelling the Evolution of Tyre Performance in a Motorsport Application

Analysis of Effects on Vehicle Performance in a Real-Time Simulation Environment

Master's thesis in Automotive Engineering

Håkan Richardson

Department of Applied Mechanics
CHALMERS UNIVERSITY OF TECHNOLOGY
Gothenburg, Sweden 2017

Acknowledgment

This thesis was made possible by Cyan Racing through guidance by Mikael Mohlin, organisation by Erik Olofsson, track support from Per Blomberg and simulator support from Christoffer Routledge, but also valuable input from the entire engineering staff. Having the opportunity to utilise the simulator facility in collaboration with their driver, Nicky Catsburg, offered an extraordinary way to evaluate the model and discuss subjective aspects of tyre performance.

Chalmers University of Technology have provided a robust academic framework with Bengt Jacobson as examiner and Anton Albinsson as supervisor. This has been a valuable source of knowledge and a great forum for discussing modelling challenges.

MASTER'S THESIS IN AUTOMOTIVE ENGINEERING

Modelling the Evolution of Tyre Performance in a Motorsport Application

Analysis of Effects on Vehicle Performance in a Real-Time Simulation Environment

Håkan Richardson

Department of Applied Mechanics
Division of Vehicle Engineering and Autonomous Systems
Vehicle Dynamics group
CHALMERS UNIVERSITY OF TECHNOLOGY
Göteborg, Sweden 2017

Modelling the Evolution of Tyre Performance in a Motorsport Application
Analysis of Effects on Vehicle Performance in a Real-Time Simulation Environment
Håkan Richardson

Master's Thesis 2017:82
ISSN 1652-8557
Department of Applied Mechanics
Division of Vehicle Engineering and Autonomous Systems
Vehicle Dynamics group
Chalmers University of Technology
SE-412 96 Göteborg, Sweden
Telephone: + 46 (0) 31-772 1000

Examiner: Bengt Jacobson, Chalmers

Supervisor: Mikael Mohlin, Cyan Racing
Anton Albinsson, Chalmers

Department of Applied Mechanics
Göteborg, Sweden 2017

Modelling the Evolution of Tyre Performance in a Motorsport Application
Analysis of Effects on Vehicle Performance in a Real-Time Simulation Environment

Master's thesis in Automotive Engineering
Håkan Richardson
Department of Applied Mechanics
Division of Vehicle Engineering and Autonomous Systems
Vehicle Dynamics group
Chalmers University of Technology

Abstract

The automotive industry use simulation tools to improve their products and increase the rate of development. In order to rely on the simulated results, robust and detailed models are necessary to capture behaviours that would be present in a real setting. This is of particular importance when models are used in driving simulators; a tool which today is considered a necessity within motorsport. The driver then need to know that the feedback provided by the model can be trusted so that realism can be maximised. From a vehicle dynamics and driving experience point of view, detailed tyre models are therefore required, since they act as the interface between vehicle and road.

In motorsport, tyres are being used at high stress levels for long periods of time, innevitably causing their visco-elastic rubber to change its properties and thereby affect overall vehicle performance. The driver needs to keep that in mind when handling the car, but also engineers when determining an appropriate suspension setup. Acquiring better understanding of how tyre performance evolve during a session will therefore aid in deriving ways of modifying its enabling factors in simulation environments.

It has been understood that it is important to not only consider degradation as abrasive wear, but also as a change of rubber damping and elasticity. Deriving ways of taking this into account was essential for it to provide accurate results.

A model consisting of seven submodels has been developed, where one is responsible for distributing the load over the width of the tyre, and one will estimate temperatures of unsprung components that affect tyre performance. The remaining five will model different physical phenomena, which come together to change the car characteristics.

It was proven that the subjective experience connected to a change of tyre performance could be replicated in a driving simulator, using the model developed as part of this thesis. The objective comparison was showing similar trends, but would require further tuning and development to reach good correlation.

Key words: Tyre, Simulation, Model, Motorsport

Table of Contents

Preface

Through the endeavour of hosting thesis projects with strong academic support from Chalmers University of Technology, Cyan Racing is commited to enhancing the vehicle development tools that allow them to remain a competitive motorsport team.

This thesis has been carried out as a partial requirement for the Master of Science degree at the Master's programme of Automotive Engineering at Chalmers University of Technology in Gothenburg, Sweden. The work has been a collaboration between university and the Chassis Engineering Group of Cyan Racing, during the period of January to December 2017.

I would like to acknowledge the extensive support provided by Cyan Racing, primarily from Mikael Mohlin, but also a word of appreciation to Erik Olofsson for accepting my thesis proposal, Per Blomberg for providing me with the opportunity to carry out measurements during a race weekend and Christoffer Routledge for enabling model validation in the driving simulator with Nicky Catsburg.

Göteborg, 2017

Håkan Richardson

Notations

Variables shown in graphs on per-corner basis will be displayed in a 2x2 grid.

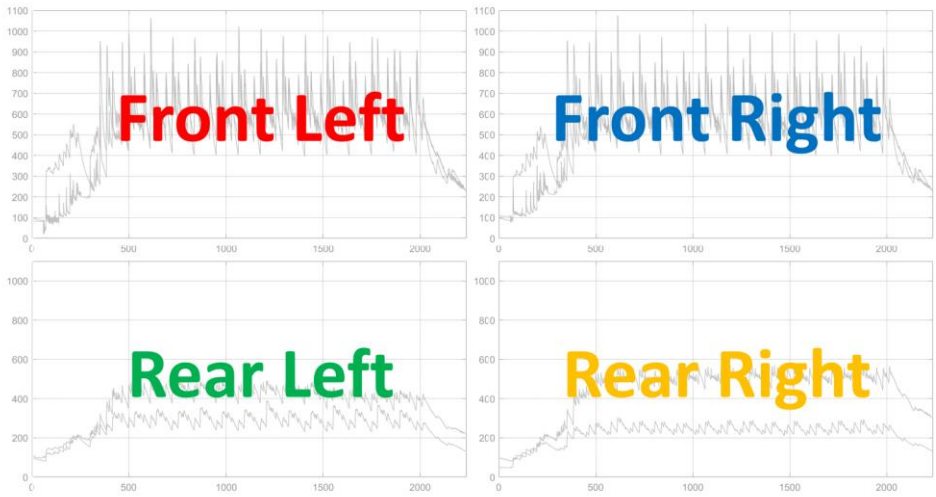

	Vehicle Dynamics	
v_{car}	Vehicle speed	[m / s]
v_{wheel}	Wheel surface speed	[m / s]
$\omega_{wheel/brake}$	Wheel angular velocity	[rad / s]
a_x	Longitudinal Acceleration	[m / s^2]
a_y	Lateral Acceleration	[m / s^2]
R	Wheel radius	[m]
w	Tyre width	[m]
λ	Tyre slip ratio	[%]
α	Tyre slip angle	[deg]
γ	Wheel camber angle	[deg]
T_g	Glass transistion temperature	[K]
F_x	Longitudinal tyre force	[N]
F_y	Lateral tyre force	[N]
F_z	Vertical tyre force	[N]
M_x	Tyre overturning moment	[Nm]
μ	Utilised total friction	[-]
μ_y	Utilised lateral friction	[-]
μ_x	Utilised longitudinal friction	[-]
C_x	Longitudinal stiffness	[N / %]
C_y	Cornering stiffness	[N / deg]
Δx	Shear length	[mm]

	Natural Constans	
σ	Bolzmann constant	[W / (m^2K^4)]
g	Gravitational acceleration	[m / s^2]
ρ	Air density	[kg / m^3]
	Surface Interaction	
y_{camber}	Camber migration factor	[m / deg]
$y_{friction}$	Friction migration factor	[m / (N/N)]
y_s	Lateral centre of pressure migration	[m]
y_p	Lateral peak pressure migration	[m]
y_d	Width of unloaded tyre segment	[m]
	Unsprung Thermodynamics	
h_{brakeF}	Front brake heating factor	[-]
h_{brakeR}	Rear brake heating factor	[-]
c_{brakeF}	Front brake cooling factor	[-]
c_{brakeR}	Rear brake cooling factor	[-]
h_{air}	Inflated air heating factor	[W / K]
c_{air}	Inflated air cooling factor	[W / K]
$h_{tyreSlip}$	Tyre slip heating factor	[-]
$h_{tyreHyst}$	Tyre hysteresis heating factor	[J / m]
c_{tyre}	Tyre cooling factor	[J / mK]
T_{brake}	Brake disc temperature	[K]
T_{air}	Inflated air temperature	[K]
p_{air}	Inflated air pressure	[bar]
T_{tyre}	Tyre surface temperature	[K]
T_{amb}	Ambient air temperature	[K]
T_{track}	Track surface temperature	[K]
	Performance Alteration	
A	Tyre wear amount	[m]
A_{new}	New tyre tread depth	[m]
A_{actual}	Actual tyre tread depth	[m]
P_{lin}	Linear range transition point	[deg]
P_{peak}	Peak grip transition point	[deg]
P_x	Longitudinal tyre force scaling factor	[-]
P_y	Lateral tyre force scaling factor	[-]

1 Introduction

Today, a significant part of automotive development is carried out in simulation environments. Here, robust and detailed models are necessary to capture behaviour which would be present in a real setting. This requires accurate tyre models to ensure that driver input is converted into appropriate vehicle motion. However, due to the flexible nature of a tyre, accomplishing this typically becomes a complex task.

Various methods exist for assigning relations between a combination of cornering, propulsion and braking demands to the appropriate amount of road-plane forces, given variables such as vertical load and wheel angles. These relations are typically of a non-linear nature and cannot be simplified without losing significant accuracy.

However, the most commonly used tyre models rarely account for a variation of performance as a result of being used close to the end of their lifecycle or outside the window of optimal temperature and inflation pressure.

A typical road car user utilises the tyre performance to such a small extent that these variations, during the span of the simulation, can be considered insignificant. This leads to a lack of models which take evolving aspects into account.

1.1 Problem Description

Within motorsport, the cars are typically driven at the limit of their performance over longer periods of time, here referred to as sessions, typically lasting between 30 and 60 minutes. In this kind of environment, the lack of models capable of reproducing change of tyre characteristics is undermining the usefulness of simulation environments.

As a motorsport team with great heritage, Cyan Racing is striving to reproduce their national domination of the touring car class in a global competition and establish Volvo as a brand of high performance. In order to achieve this, they are continuously investigating ways in which to develop their cars to maximize track performance.

The cars are designed to utilise the tyres in the most efficient way possible. While current models offer a good basic understanding of the tyre characteristics, simulations which last entire sessions lack detail of changes in performance over time.

1.2 Objective

The objective is to acquire greater understanding of how tyre performance evolve during a normal session and build a model capable of reproducing this behaviour in a real-time simulation environment.

1.3 Solution

Using an extensive set of data logged by the cars of Cyan Racing during sessions, causes of tyre performance evolution were derived. The data included signals such as car body accelerations, tyre temperatures, inflation pressure, vehicle speed, driver inputs and road conditions.

The different causes were then quantified and compared to allow for a greater focus on key aspects. Through this, a tyre evolution model was derived, capable of replicating the change of tyre performance as a function of the current and previous vehicle states. The model has been created by taking a physical approach and combining that with empirically derived scaling factors that aid in matching the overall vehicle performance.

1.4 Deliverables

The thesis come with the following deliverables:

- A process of how to derive parameter values for a tyre evolution model using logged data.
- A tyre degradation model capable of replicating tyre evolution in such a way that a real-time simulation would show similar trends to those of the real car.
- Model validation through subjective assessment by professional driver in a driving simulator and objective comparisons with logged vehicle data.
- A detailed report covering the modelling approach and utilisation of the tyre degradation model.
- An MSc thesis which meets the requirements of both Chalmers as an academic institution and Cyan Racing as an industrial stakeholder.

1.5 Limitations

The following limitations have been identified for this thesis:

- Degradation as a result of normal aging will not be considered, only degradation which is caused by usage of the tyre.
- Only dry asphalt and the tyre used by Cyan Racing will be considered throughout analysis and modelling.

2 Scope

To maximise the output quality of the project, a set of prerequisites has been applied based on time frame and desires of the stakeholders.

2.1 Car

The vehicle used as the basis for this project is the Volvo S60 Polestar TC1, competing in the World Touring Car Championship. It is a front-wheel driven car designed by Cyan Racing, featuring a turbo-charged race engine based on the Volvo Drive-E engine platform.The car is displyed in Figure 1 and its specifications can be found in Table 1.

Table 1 – Specifications of the Volvo S60 Polestar TC1

Specification	Value
Driven Axle	Front
Peak Power	400 BHP
Peak Torque	450 Nm
Nominal Weight	1200 kg

Figure 1 – Appearance of the Volvo S60 Polestar TC1

The car is equipped with sensors for various purposes, but the ones used in this thesis has been included as red parts in Figure 2. The one in the middle of the car is measuring vehicle motion (v_{car} , a_x , a_y) while the ones in each wheel measure the thermal state of unsprung components (T_{brake} , T_{air} , p_{air} , T_{tyre}). The latter sensors and signals are further demonstrated in Figure 3.

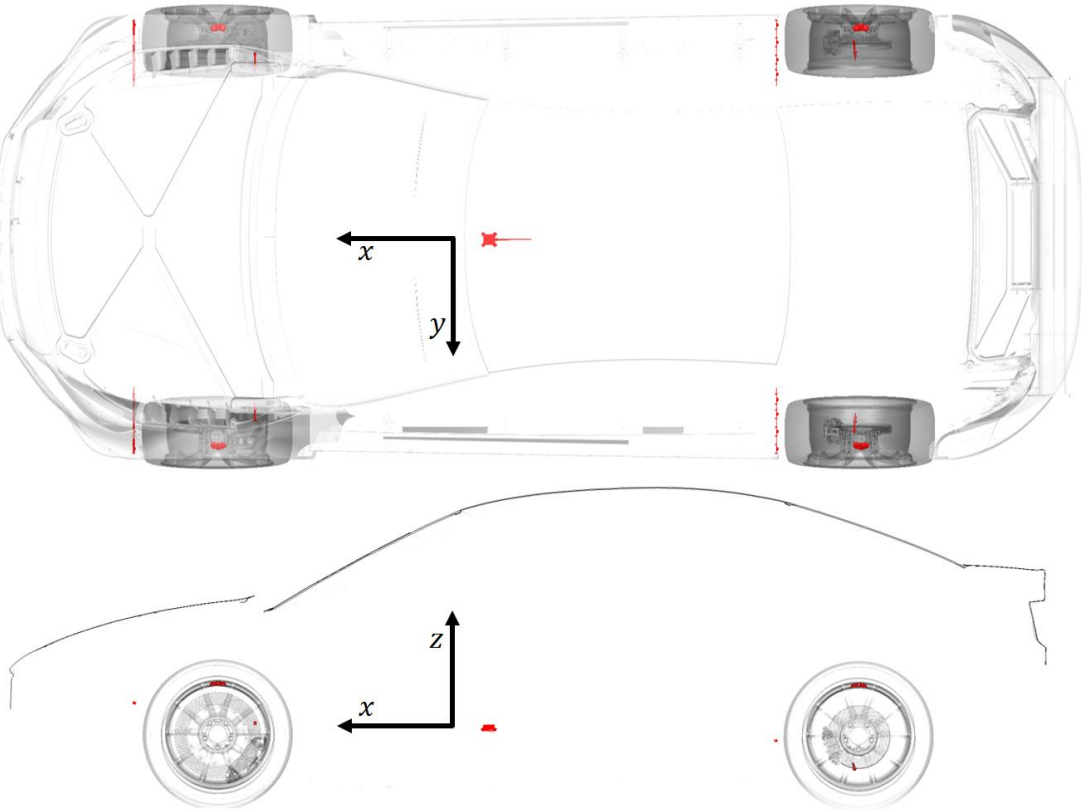

Figure 2 – Top and side view with coordinate system and red marked sensors

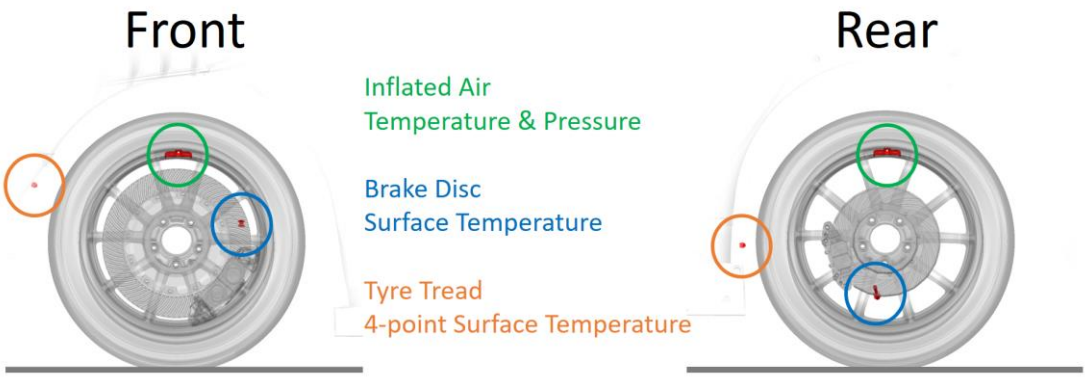

Figure 3 – Sensors in the unsprung components

2.2 Tyre

The tyres used on all cars competing in the World Touring Car Championship are called *Yokohama Advan A005 250/660 R18*. No specification is available from the manufacturer, but Cyan Racing has carried out isolated rig tests to better understand the tyre performance. When data is stored after a test, the coordinate system of Figure 4 is employed. Sensors for temperature and pressure were mounted in a similar way to the car, allowing for comparisons between the two cases.

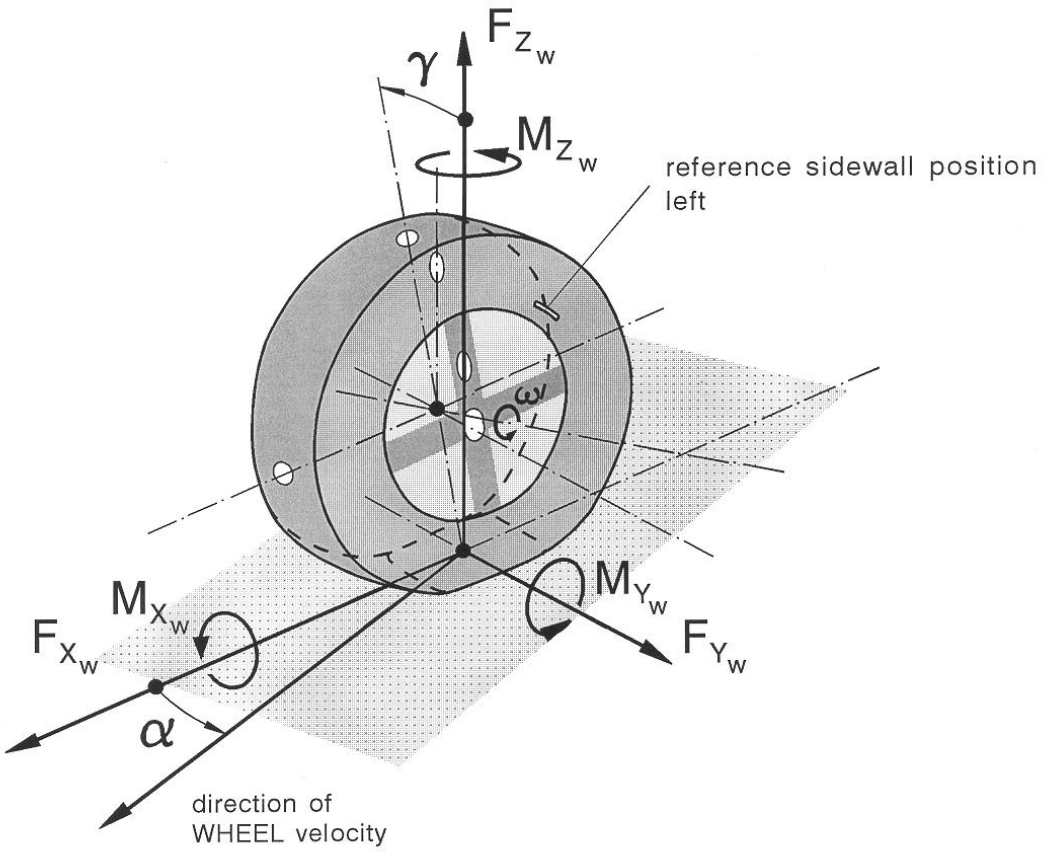

Figure 4 – Tyre coordinate system (x = forward, y = left, z = up)

2.3 Tracks

The car has been driven on multiple tracks over the course of a year, but the ones with more unique characteristics and comprehensive data sets will be used as the foundation of the thesis. They feature different ambient air and track surface temperatures, but have all been driven in dry conditions.

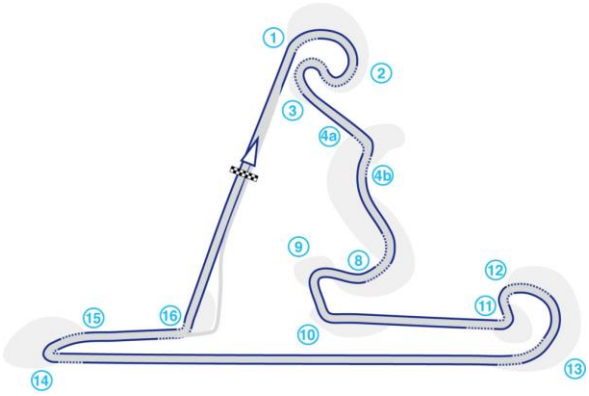

Figure 5 – Shanghai International Circuit

The circuit displayed in Figure 5 is located in Shanghai, China and features two long straights. The first one leads into turn 1 and 2 which are renowned for how their length damage the tyres, just before the car enters the faster corners of the track. The second long straight leads into the heavy braking zone of turn 14, putting a great deal of stress into all unsprung components.

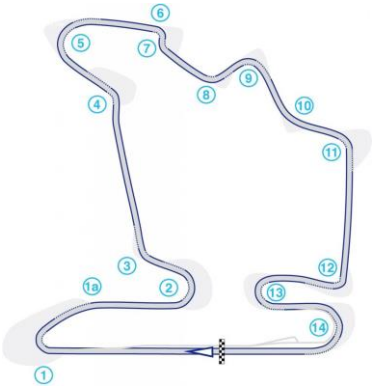

Figure 6 – Hungaroring

Figure 6 shows the layout of Hungaroring, located outside the Hungarian city of Budapest. It has many heavy braking zones ahead of its 180 degree corners, putting a great deal of slippage into the tyre during propulsion phases. The fast middle sector requires good corner entry behaviour and car balance to set quick laptimes.

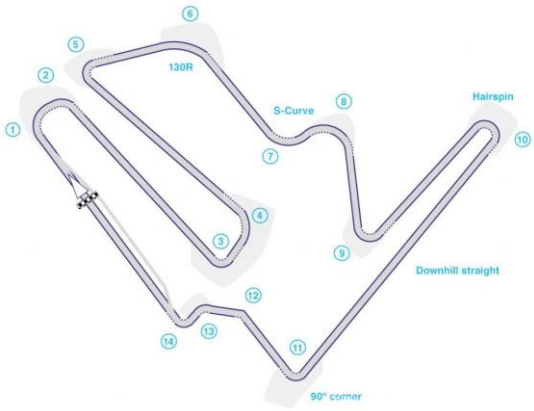

Figure 7 – Twin Ring Motegi

The Japanese track of Twin Ring Motegi features many long straights as seen in Figure 7. Due to hot conditions during the weekend, all unsprung components are being pushed to their limit. While the number of corners is at a normal level, the actual cornering difficulty is significantly fewer than for other tracks on the calendar, putting more emphasis on braking performance.

3 Theory

The primary method of evaluation for this thesis was set to be subjective assessment. Part of the knowledgebase used to drive the project forward has therefore come from the experience of drivers and engineers within the team. This has offered insight into which aspects of tyre performance evolution that are to be prioritised, but also identification of trends which require extensive on-track experience. This has then been combined with existing research within the field of tyre modelling and logged data from both car and testing rigs.

3.1 Tyre Fundamentals

The tyre is the sole point of interaction between ground and vehicle. While a rubber compound acts as the final interface towards the texture of the track, its performance is also affected by various mechanical re-inforcements and chemical additives, working to offer good manouverability to the driver. A classic approach to the concept of friction dictates that the maximum in-plane force is proportional to the normal load, independent of the contact area. While this holds true in several engineering applications, it does not explain the workings of a tyre.

Upon driver input, lateral or longitudinal, the tyres will experience deformation caused by velocity differences between rubber and track surface. This gives rise to a reaction force which allow the car to perform desired manoeuvre.

The performance capabilities of the interface is largely affected by the properties of the rubber material, which in turn is evolving as it is being subjected to mechanical and thermal stress. Some of these phenomena are reversible, meaning that there is an ideal window of operation, while some are irreversible in terms of how they affect the performance of the tyre.

3.1.1 Utilisation

Upon wheel rotation, new parts of the rubber surface reach the track. Based on its speed difference compared to the ground and the properties of the material, it will either stick and be skewed as it travels along the length of the contact patch, or slide as the sticking fails. The first range is known as the elastic and the latter is known as the frictional range. A combination of the two is known as transitional, occurring as the reaction force of the skewed rubber reaches its maximum capactity before the end of the contact patch. This scenario is demonstrated in Figure 8 in the case of longitudinal slip under braking. The product of wheel angular velocity ω_{wheel} and the wheel radius R is equal to the tyre surface tangential speed v_{wheel}. Its relation to the speed of the vehicle v_{car} is defined as the longitudinal slip ratio λ, described in Equation (3.1).

$$\lambda = \frac{v_{wheel} - v_{car}}{v_{wheel}} \quad , \quad v_{wheel} = \omega_{wheel} \cdot R \qquad (3.1)$$

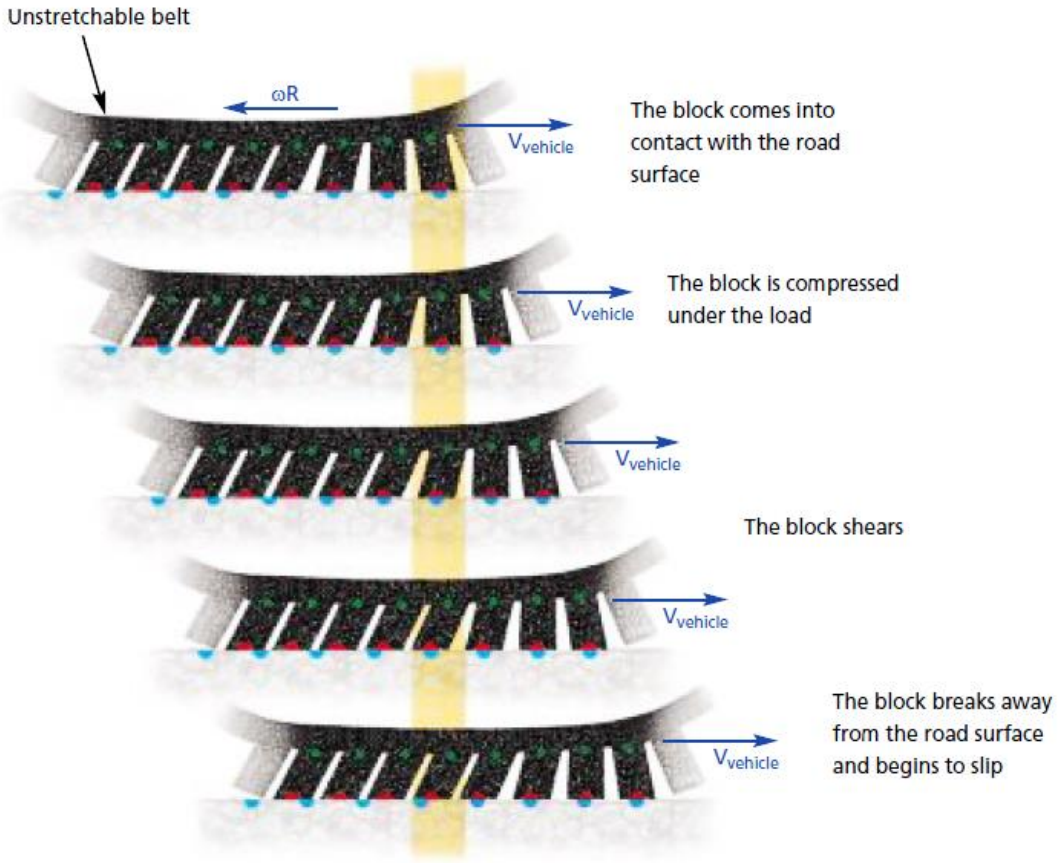

Figure 8 – The rubber is skewed before it starts to slip (Michelin, 2001)

The same holds true for cornering manoeuvres. Upon steering input, the wheel's plane of rotation is mis-aligned with the trajectory of the wheel path. Their angular offset is known as the slip angle, as seen in Figure 9. It gives rise to a lateral skewing of the contact patch, similar to the one of longitudinal cases.

Upon reaching the maximum elastic capacity of the tyre, any remainder of the rubber which is still in contact with the ground will start to slide. The tyre has then moved into the transitional range, potentially ending up in the frictional range of full sliding, displayed in Figure 10. The slope of the initial elastic range is covered in Section 3.2, and is known as the cornering stiffness; a key factor when discussing the driving experience (Milliken & Milliken, 1995).

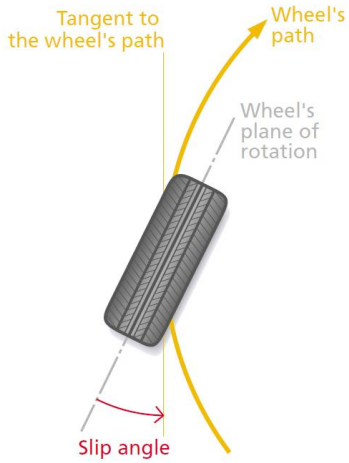

Figure 9 – Definition of the slip angle (Michelin, 2001)

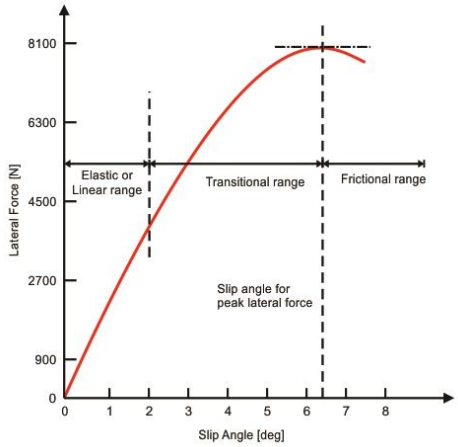

Figure 10 – Lateral force vs slip angle (Milliken & Milliken, 1995)

When there is a combination of lateral and longitudinal demands, the maximum grip in each direction is lower than under pure slip in one of the directions. To simplify the behaviour, the term *friction circle* is commonly used where it is assumed that the maximum total force stays the same, independent of it containing both lateral and longitudinal components, as shown in Figure 11.

Figure 11 – Longitudinal slip will negatively affect lateral grip

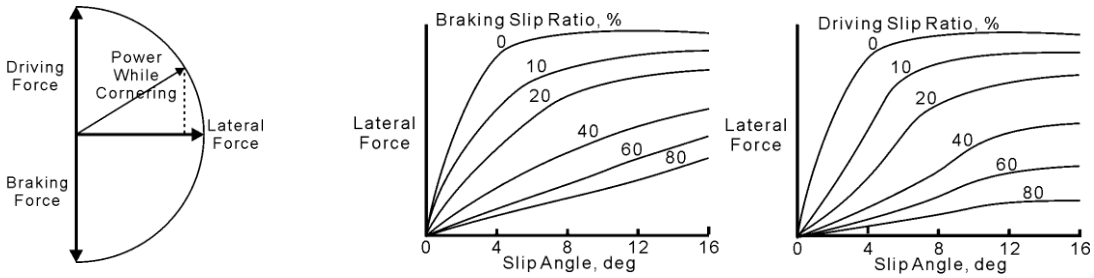

Figure 11 – Longitudinal slip will negatively affect lateral grip (Haney, 2003)

3.1.2 Construction

The tyre is a rubber construction, significantly re-inforced by metal and composite materials. It can be split into four distinct regions, each with its own function and structure, as seen in Figure 12.

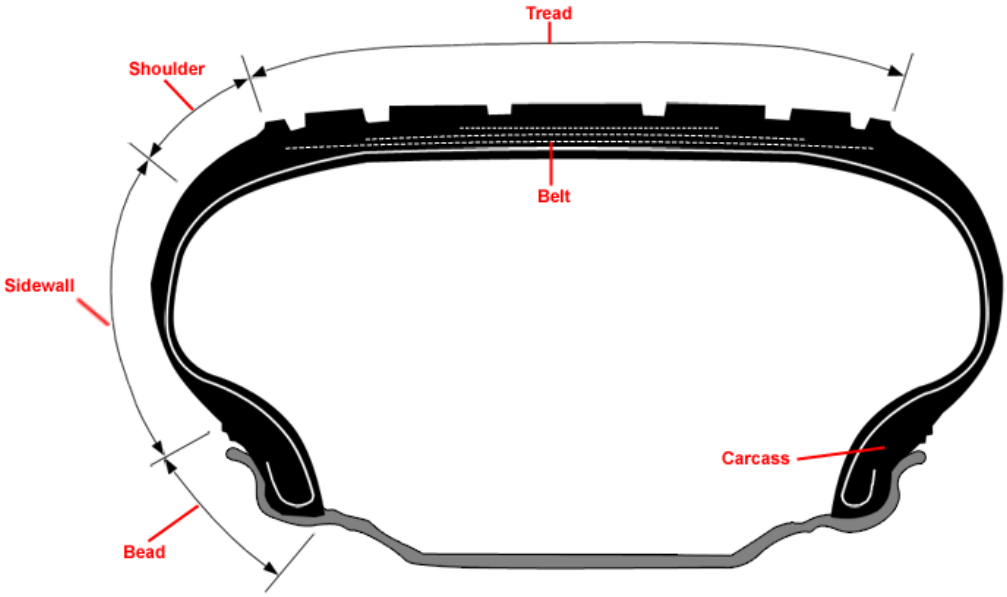

Figure 12 – The construction of a tyre (RD, 2017)

- The **Tread** is the interface towards the ground. In motorsport applications on dry tarmac, tyres known as slicks are typically used, meaning that this surface does not have any grooves. It is made from a soft rubber compound, allowing it to wrap around road asperities and therefore maximise grip. It is supported by **Belts** in different materials which ensure responsiveness and maintained structural integrity of the outer rubber layer.

- The **Shoulder** is a rubber segment primarly used to protect and reduce stress concentrations between the different plies in that part of the tyre. It is not the primary contact patch, but may experience stress in during strong manoeuvres.

- The **Sidewall** is the interface between a relatively stiff outer belt and the rim, ensuring that the tyre can contain its inflation pressure and will therefore play a significt role in the overall stiffness.

- The **Bead** acts as the anchoring system of the tyre. It houses steel wires which wrap around the rim, preventing it from sliding off. The **Carcass** is made out of thin steel cords and a sealing layer which wraps around the whole tyre.

Due to the construction of the tyre, it cannot take vertical loads without being inflated. The side walls are primarily designed to be in tension, resulting in that some of the vertical force will be transmitted via the inflated air to the upper part of the tyre. This makes the carcass deform in an attempt to expand, but instead stay intact due to the anchoring of the bead. This load path is demonstrated in Figure 13.

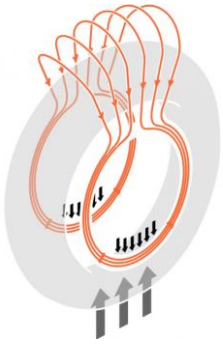

Figure 13 – Tyre vertical load path (Wright, 2017)

However, car tyres vary in the amount of mechanical reinforcements that are being used, as covered in Section 3.2.2. Upon vertical compression of a tyre with strong mechanical structure, the sidewalls will exert a greater vertical component of the force F_a below than above the rim, resulting in a net upwards force (Guiggiani, 2014).

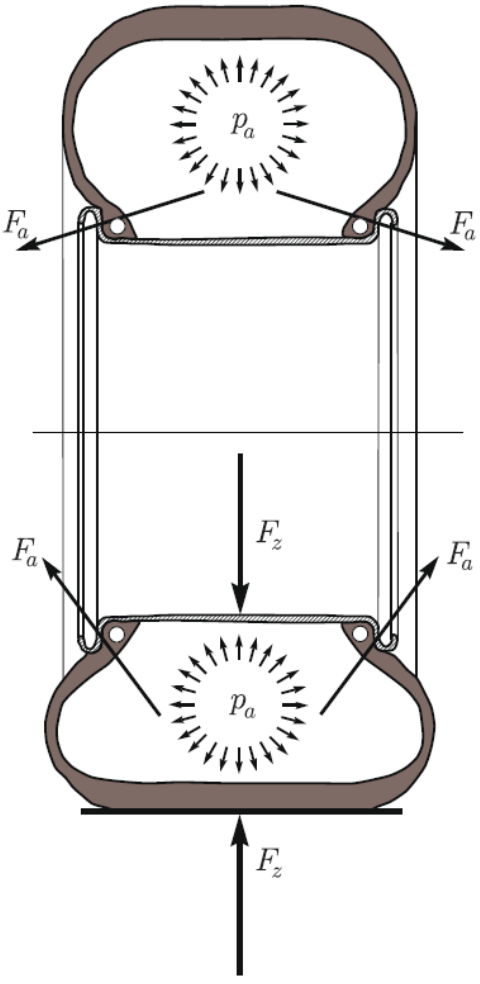

This is demonstrated in Figure 14, where p_a corresponds to the tyre inflation pressure. Excessive loading of the sidewalls can cause critical failures, so it's important to ensure good support from the air.

The bias between these phenomena is determined by the inflation pressure, so tyre manufacturers supply teams with pressure guidelines to prevent sidewalls from being damaged upon heavy usage (Cyan, 2016).

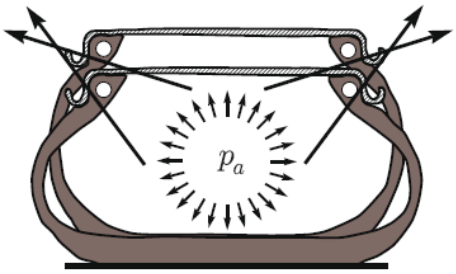

Figure 14 – Vertical compression of tyre (Guiggiani, 2014)

3.1.3 Materials

Rubber is a soft, virtually incompressible material with visco-elastic properties, meaning that when it is stretched and released it will return less energy than what was put into the material. This is due to its molecular structure of flexible coils. Their chemical crosslinks consist of sulphur bridges, formed through a process known as vulcanisation (Gent, 2007). As these coils move, they rub against each other, giving rise to the viscous damping behaviour of the rubber. The amount of sulphur bridges increase the further into the vulcanisation process the rubber reaches, lowering the damping effect of the material (Michelin, 2001). This has an extensive impact on the grip, as covered in Section 3.3.1, and is reason for carefully managing time and temperature during the manufacturing of the tyres (Menneglier, 2017).

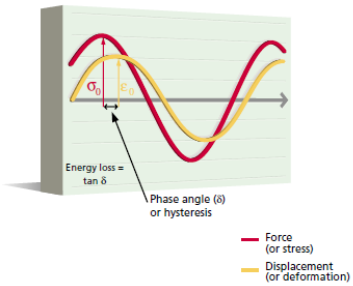

Upon deformation of a purely elastic object, the strain will be in phase with the stress. However, when deforming a visco-elastic material the strain lags behind the stress with the phase angle δ. This is known as hysteresis and demonstrated in Figure 15.

Figure 15 – Visco-elastic phase lag between stress and strain (Michelin, 2001)

As deformation is imposed through a given excitation frequency, the amount of hysteresis will be dependant on the temperature of the rubber. This phenomena is described through the WLF *(William Landel Ferry)* equation. For the rubber of tyres, it can be approximated that increasing the excitation frequency by a factor of 10 equates to a drop in temperature of 7 to 8 ℃ (Michelin, 2001).

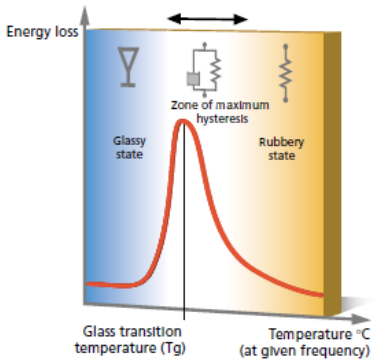

Above the glass transition temperature T_g, the material is in a rubbery state, while below it will have glassy characteristics (Gent, 2007). Tyres used in motorsport typically have a significantly higher T_g compared to that of a road car tyre, allowing for usage in a higher optimal temperature range (Farroni, Russo, Riccardo, & Timpone, 2014). It is around T_g where the rubber will offer maximum hysteresis, seen in Figure 16, since the rubber has then left its brittle range, but will still be rigid enough to dampen its elasticity (Michelin, 2001).

Figure 16 – Hysteresis in the rubber over two temperature ranges (Michelin, 2001)

3.1.4 Modelling

The standard definition of friction is not sufficient to accurately model the behaviour of a tyre. Instead various approaches to describe force generation in relation to tyre slip are employed; each with their own strengths and weaknesses.

In essence, they are either based upon fitting a model to data from dedicated tests with the real tyre, or attempting to model the underlying physical phenomena that give rise to forces as the tyre is being subjected to input from the driver.

Due to the computational complexity of the latter case, model fitting is the most common approach in real-time simulation applications. In cases such as highway driving where limit handling behaviour is not evaluated, it is sufficient to describe the tyre characteristics as producing the same amount force per slip unit, intependendent of its magnitude. This is known as a linear tyre model, demonstrated as a blue line in Figure 17. The slope is known as the stiffness; C_x in a longitudinal case and C_y in a lateral case. A slightly more complex model would limit the maximum force by ensuring that the available friction level is below a certain threshold, typically between 0.8 and 1.8 depending on surface conditions and tyre characteristics. This version of the linear model is shown in Equation (3.2).

$$F_y = min(\, C_y \cdot \alpha \quad , \quad F_z \cdot \mu \,) \tag{3.2}$$

A non-linear model allows for better correlation between test data and model output, while still requiring relatively low computational effort. A typical example of such model is the Magic Formula (Pacejka, 1992), whose output is demonstrated as the red line in Figure 17. The grey dots correspond to raw data from a tyre testing facility.

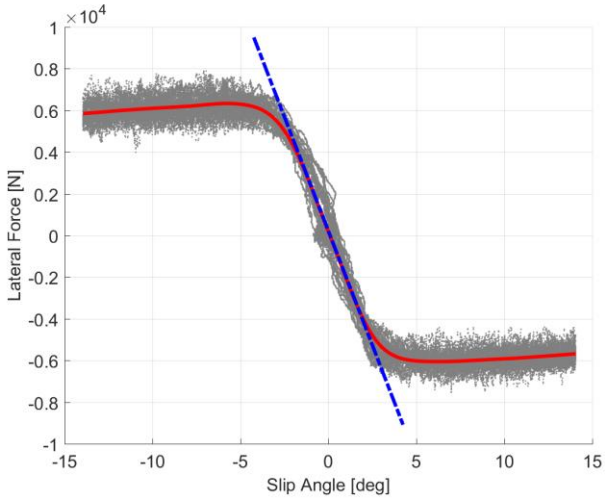

Figure 17 – Tyre testing data with different model fitting solutions (Cyan, 2016)

In a motorsport application, limit handling characteristics is of great importance, rendering the linear models insufficient. It should be noted the even the more complex linear model with force saturation will neglect *load sensitivity*, which is one of the key tyre properties that will affect design of the vehicle onto which the tyres are fitted.

It describes how the peak available friction μ is not constant, but dependant on the vertical force that is being put onto the tyre. This can be seen in Figure 18, where grey dots correspond to tyre testing data and the red line is added to highlight this phenomena. The cause of this will be discussed in Section 3.3.2.

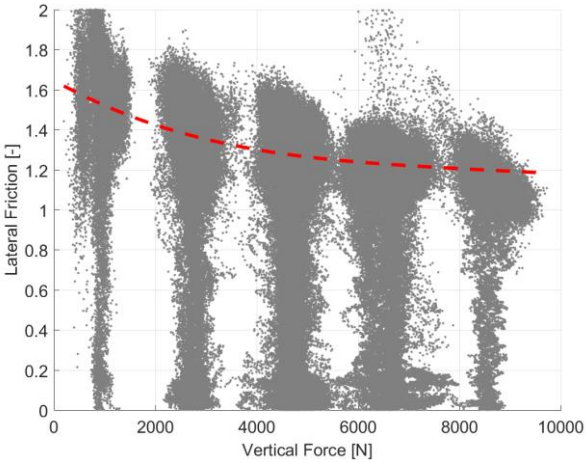

Figure 18 – Peak available friction drops when vertical load increase (Cyan, 2016)

Certain aspects must be incorporated in a good tyre model that is to be used in a motorsport application, especially in a driving simulator.

- Transition from linear grip build-up to non-linearity around the peak.
- Friction limits dependending on vertical load.
- Loss of grip upon excessive slip.
- Grip change due to camber.

3.1.5 Response

As tyres are the only way to transfer forces between vehicle and ground, changing their characteristics will inevitably affect the dynamic behaviour of the car and its reponse to driver input. Race tracks offer a great amount of variations, but can be generalised to easier connect vehicle response to a certain phase of cornering or acceleration.

It was understood that drivers are primarily able to sense a change in yaw balance and the transient response that accompanies an input of the driver. As for the absolute level of grip, sensing the magnitude of sustained road-plane accelerations is typically difficult, but tend to be reflected in change of lap and sector times (Catsburg, 2017).

The sensation of altered tyre performance is most prominent in situations of combined lateral and longitudinal slip. This is primarily occurring in the late stages of the corner where the driven axle, in this case the front, will lose lateral grip due to the propulsion demand of the driver (Catsburg, 2017).

3.1.6 Support

The tyre is supported by inflated air, encapsulated by a slipping rubber surface and a rim that is situated close to a hot brake disc. These elements make it inevitable for the air to be heated during the course of a race, resulting in a rising pressure. Sidewalls and carcass require a certain inflation pressure to maintain structural integrity during high stress, but over-inflation will cause a limited contact patch, as seen in Figure 19.

Figure 19 – The inflation pressure will affect the footprint (Tyrecity, 2017)

To manage this phenomena and maximize the overall tyre performance, the inflation pressure before the session is set lower than the ideal level to allow for expansion as the race progress. A thermal equilibrium is reached after the first laps (Mohlin, 2017), as seen in Figure 20.

The driver has access to a readout from pressure sensors in the wheel, informing them about the current pressure levels. This allows them to adjust the amount of stress they put into the tyres accordingly (Catsburg, 2017).

The hot air will also contribute to heating the inner surface of the tyre, which eventually will increase the core rubber temperature.

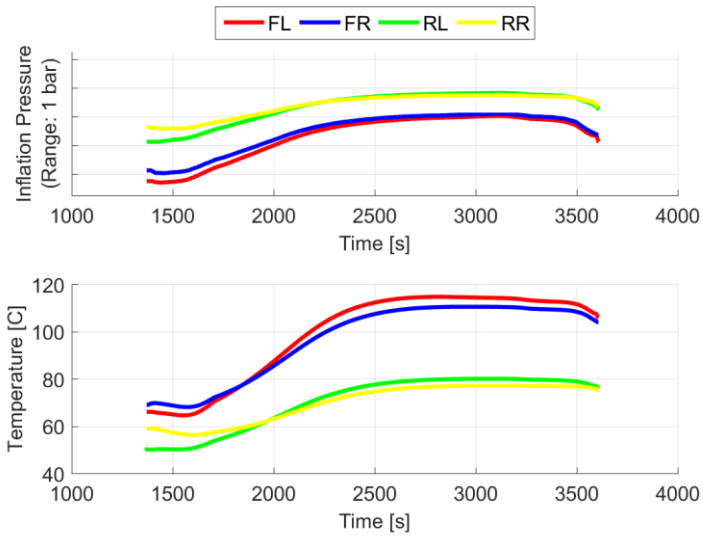

Figure 20 – The inflated air will change in temperature and pressure (Cyan, 2016)

3.2 Stiffness Mechanics

Before reaching peak attainable grip, the rate of force generation per input slip is known as tyre stiffness. It plays a significant role in how the vehicle responds to small steering input or the initial phase of a larger input.

The lateral force that makes the car turn originates from the tyres' ability to counteract lateral deflection, demonstrated in Figure 21. This process can be considered as two elements in shear; one container of pressurised air and one rubber block.

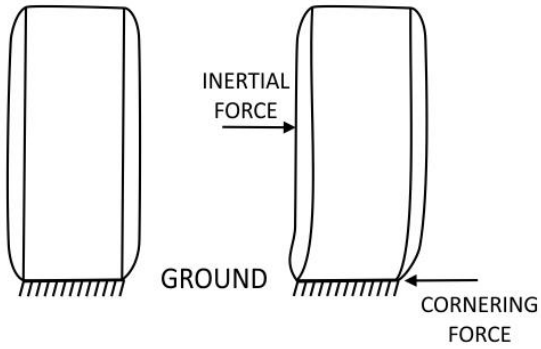

Figure 21 – Tyre deflection is induced by the cornering force (Santos, 2014)

The air container is made up of the rim and inner surface of the tyre. Low inflation pressure will result in a lower reaction force per given defomation and therefore offer a less agile cornering performance. The rubber block is what's known as the tread and for a road car, its depth is much greater than for a racing tyre. It has been theorised that this may be one cause behind the lower stiffness of a road car tyre, giving reason for further investigation of the relation between tread depth and cornering stiffness.

As the tyre rotate, any given part of it that comes in contact with the ground during a cornering manoeuvre will travel along the path similar to one marked with a red line in Figure 22. As it reaches point B, the level of reaction force will be dictated by the above mentioned phenomena. After this point the local friction and load is not sufficient to keep the tread block stuck to the road and it will therefore start to slip towards point C.

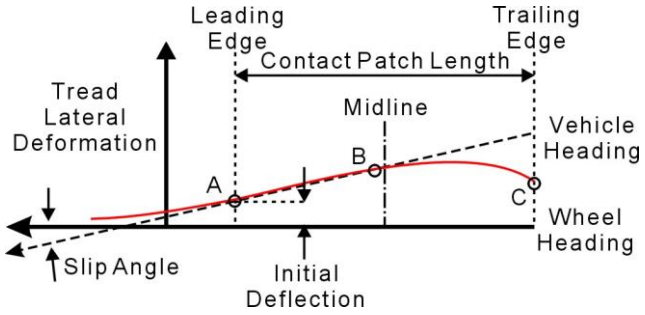

Figure 22 – A rubber block travels along the contact patch (Haney, 2003)

3.2.1 Tread

Shear modulus G for a rubber block is defined according to Equation (3.3). The surface area T_{area} is assumed constant and operation is carried out below the interfacial grip limits of tyre and road, so that no sliding occurs.

$$G = \frac{F_y \,/\, T_{area}}{\Delta x \,/\, A_{actual}} \tag{3.3}$$

If stiffness is defined as the amount of lateral force produced per unit of road-plane skewing according to Equation (3.4), it can be understood that the stiffness increase as the tread wears thinner. The parameters are illustrated in Figure 23.

$$\frac{F_y}{\Delta x} = \frac{G * T_{area}}{A_{actual}} \tag{3.4}$$

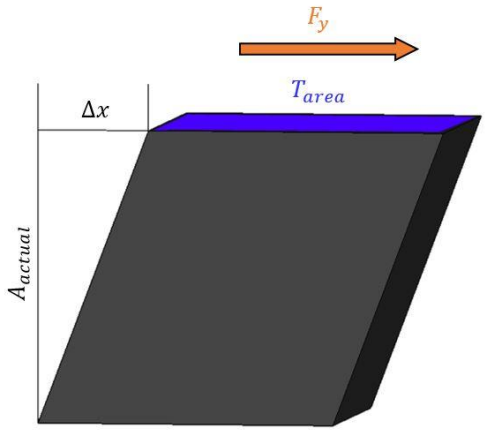

Figure 23 – Non-Linear shear compared to linear shear

No research on the topic of stiffness in relation to tread depth has been found, so the only foundation is experience of road car tyres. It should be noted that the tyre depth of a new tyre, A_{new}, is significantly larger for road cars compared to race cars, demonstrated in Figure 24. Common depths are 8 – 12 mm and 2 – 4 mm respectively. This may render the effect insiginificant, but will still be evaluated through test data.

Figure 24 – The depth of a new tyre is different for road and race cars

3.2.2 Inflation

The inflated air is used to support the tyre construction. Under-inflation will make the tyre collapse or offer a sub-optimal load distribution over the contact patch, which may lead to excessive wear and failures.

For a *'structural'* tyre with strong mechanical construction, the air play a less significant role in the overall stiffness, but is still necessary to make the tyre useful. Tyres which are *'balloon-like'* will be more pressure sensitive.

A loaded tyre will be compressed. Upon lateral input, the tyre will be deformed, giving rise to a counteracting force, demonstrated in Figure 25. For a low inflation pressure the rate of force build-up will be low, but may rise as the pressure goes up.

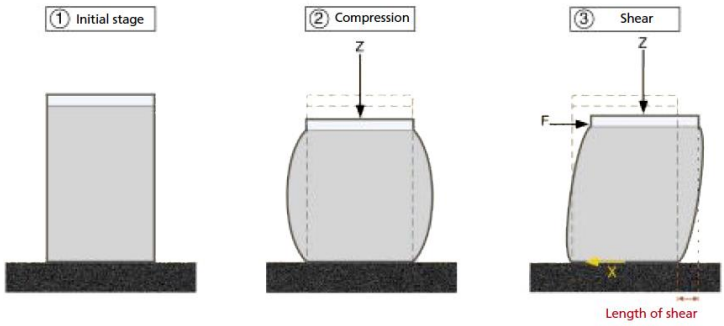

Figure 25 – Tyre deformation upon lateral force (Michelin, 2001)

The tyre which has been used by Cyan Racing is a relatively *'structural'* tyre, meaning that the inflation pressure will have less effect on the overall stiffness compared to a *'balloon-like'* tyre (Mohlin, 2017).

3.3 Grip Mechanics

When the tyre surface is pressed onto the track, its ability to stay in contact with the ground will dictate how much road-plane stress that can be put into the tyres and thereby limit longitudinal and lateral accelerations of the car. The grip of a racing tyre can be split in two parts; hysteresis and adhesion (Haines, 2011) (Wright, 2017).

In order to understand these phenomena, the surface onto which the tyre is placed must be taken into account. Typical tarmac contains various wavelengths, demonstrated in Figure 26. Wavelengths in the range of 0.001 – 0.1 mm are classified as micro roughness and those in the range of 0.1 – 10 mm as macro roughness (Michelin, 2001).

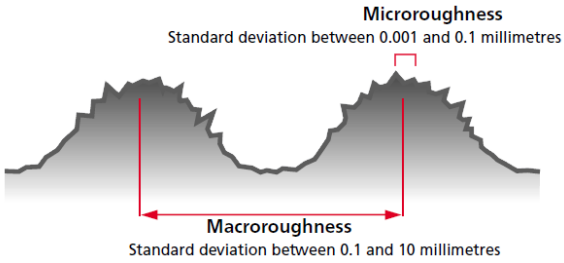

Figure 26 – Tarmac contains various wavelengths (Michelin, 2001)

Each class of wavelengths can exist to various extents within the same surface, as seen in Figure 27, resulting in diffent challenges when attempting to maximize grip. Lower wavelengths will generate higher excitation frequencies for a given slip speed between tyre and road (Persson B. N., 2014).

Adhesion: The flexibility of the tyre will allow it to wrap around the larger asperities of the road surface, creating an effective area of contact in which chemical bonds between rubber and asphalt will be formed.

Hysteresis: As the asperities penetrate the rubber, its visco-elastic properties result in energy dissipation within the material. This cause a higher net pressure on the upstream side of the asperity and thereby a force which counter-act slippage.

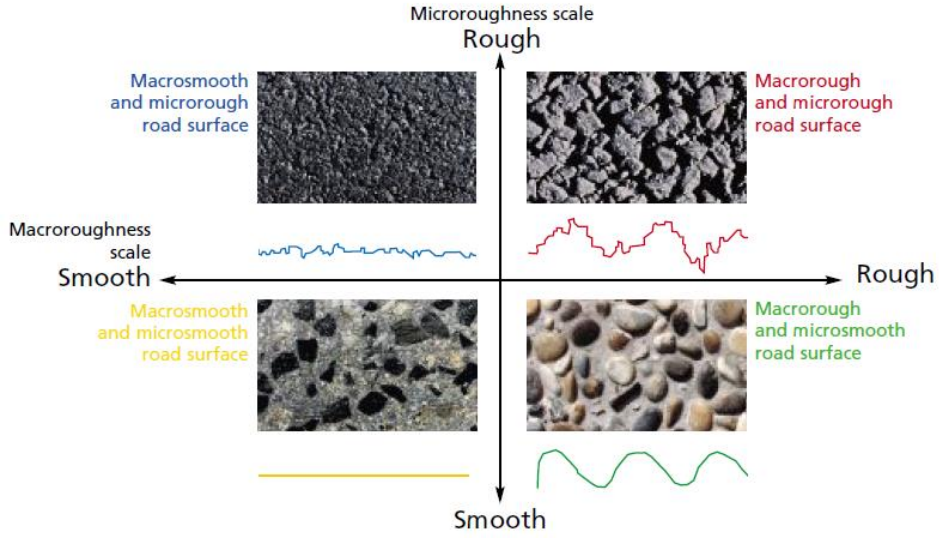

Figure 27 – Varying levels of the different wavelength classes (Michelin, 2001)

The overall grip contribution for each of these phenomena can not be generalised for all driving situations. However, adhesion is significantly decreased in wet conditions due to fluids preventing ground contact (Haines, 2011), as covered in Section 3.4.2.

Both phenomena are highly affected by the visco-elastic properties of the rubber which in turn is a function of stress frequency and core temperature (Haines, 2011). This since it affects both the ability for rubber to maximise area by wrapping around asperities and its hysteretic response to penetration (Persson B. N., 2014). The two components of grip are demonstrated in Figure 28.

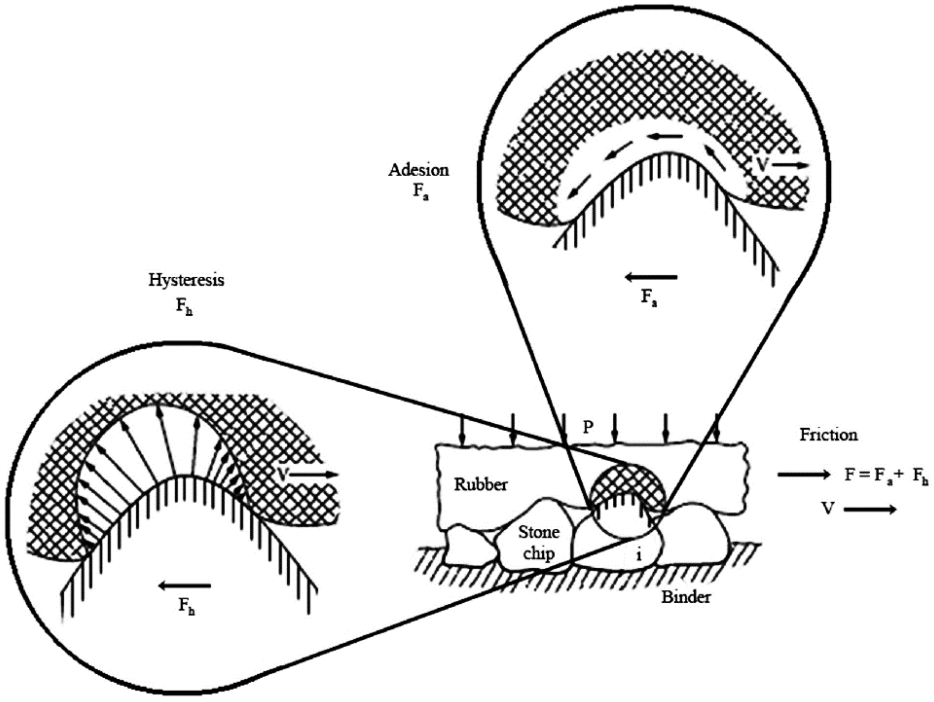

Figure 28 – Hysteresis and adhesion (Farroni, Russo, Riccardo, & Timpone, 2014)

An approach of superposition is demonstrated in Figure 29. When disregarding the interconnected nature of adhesion and hystereis, one can easier quantify the effects of each wavelength in the track surface (Farroni, Russo, Riccardo, & Timpone, 2014).

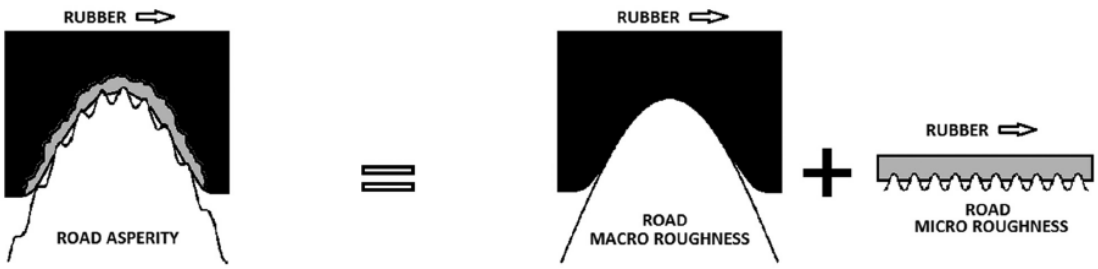

Figure 29 – Grip superpositioning (Farroni, Russo, Riccardo, & Timpone, 2014)

3.3.1 Hysteresis

When the tyre surface is penetrated by an asperity, it will absorb more energy during the loading phase compared to what's released during the unloading phase (Haney, 2003). This is caused by the structure of the material, as covered in Section 3.1.3. The rubber eventually recovers its original shape, but along the load path of Figure 30.

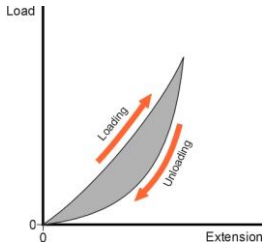

Figure 30 – The load path of a hysteretic material (Wright, 2017)

For simple vertical loading and unloading, this would not introduce any horizontal forces. However, when combining this with relative movement between ground and tyre as in the case of driving, the pressure will be higher on the upstream face of the asperity. That is due to it being the area which undergoes loading, while the downstream face will experience a lower pressure due to the dissipation occuring during unloading. This is demonstrated in Figure 31 and is the reason behind hysteresis being desireable when producing the net horiszontal force known as grip (Wright, 2017).

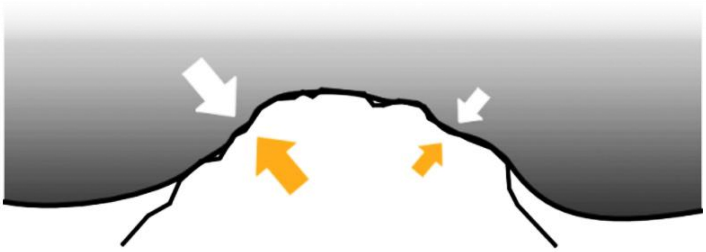

Figure 31 – Load distribution over an asperity (Wright, 2017)

The grey area of Figure 30 corresponds to the energy that has been dissipated into the material in the form of heat, contributing to a speed dependant temperature build-up in the core of the rubber (Wright, 2017). This and other heating phenomena will affect the hysteretic response for the next loading cycle.

When the tyre gets hotter, the visco-elastic spectrum of the rubber shifts so that it takes higher frequencies to reach the same hysteretic response (Persson, Tartaglino, Albohr, & Tosatti, 2005). For a given road texture, this would require higher speed, which may not be possible due to limitations in grip. This is the vicious circle a race car risk to enter when overheating the tyres. As described in Section 3.1.3, the heat then ends up vulcanising the tyres at an excessive rate, adding to the loss of grip.

3.3.2 Adhesion

The adhesion component of grip is based on temporary *van der Vaals* bonds between tyre and road surface. In order for them to be formed, the tyre needs to be in close contact with the ground, which means that the elastic properties must allow the rubber to match the road irregulaties. When this occurs, the bond can be formed, allowing it to be stretched and therefore help the tyre to resist skidding. The bond will then break, allowing it to form again at a later stage (Michelin, 2001), as seen in Figure 32.

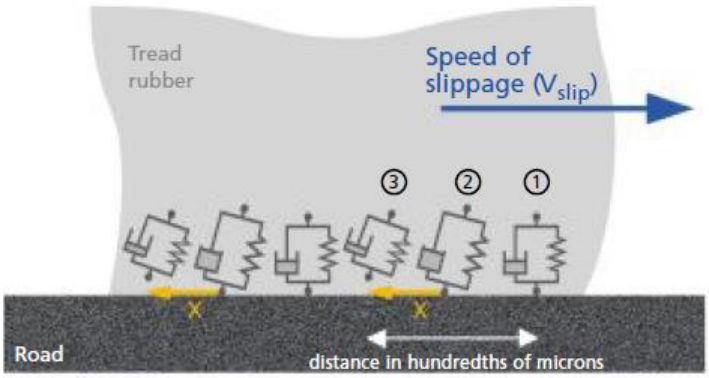

Figure 32 – Bonds are formed between road and tyre (Michelin, 2001)

The classic approach to friction between surfaces dictates that the maximum in-plane force is independent of the contact area. This only holds true for materials where the effective area of contact can be considered unrelated to the vertical load. In the case of rubber on a surface with irregularities, the area is increased when load is applied, demonstrated in Figure 33. However, it does not increase proportionally (Wright, 2017), giving rise to the load degressive phenomena of Figure 18.

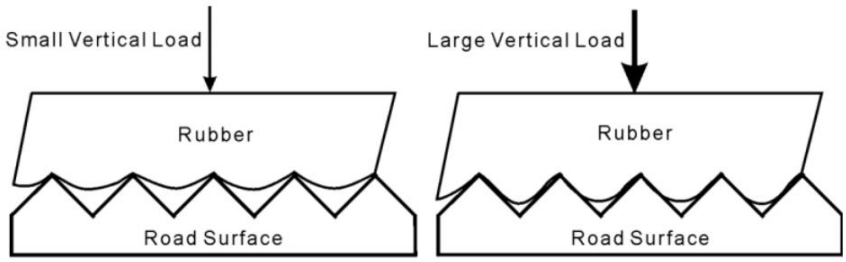

Figure 33 – The tyre contact area depends on the vertical load (Veen, 2007)

3.4 Road Interface

In order to maximise the potential of adhesion, interfaces between tyre and road should be free from particles that may limit the area of contact as the tyre is rotating. This includes fluids between the asperities of the road, but also debris and dust which may be stuck to the tyre surface.

Due to the limitations of this thesis, no extensive effort has gone into understanding this grip-limiting factor, but it is still an important aspect of tyre modelling in a motorsport application.

3.4.1 Debris

Contamination from debris or dust will limit the available surface area for interaction between road and tyre. This has an effect on all grip mechanics, but its significant impact arise through instability.

Due to its uneven distribution the tyre will start to oscillate vertically, giving rise to lower net grip, but also vibrations in the steering system. This will have a negative effect on the drivers' ability to judge the dynamics of the car and therefore result in either an issue of safety or a lack of performance (Catsburg, 2017). A typical tyre surface after a session may appear as in Figure 34.

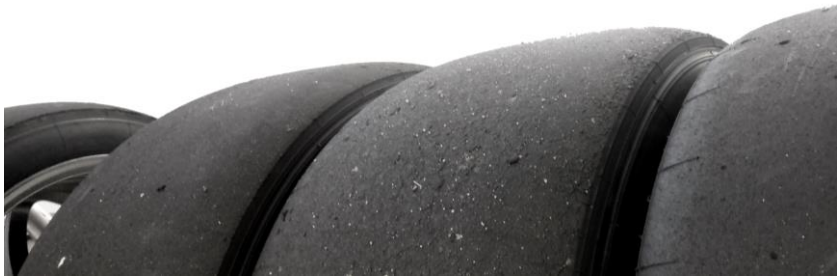

Figure 34 – Tyre surfaces with various levels of debris after a session

3.4.2 Rubber

The asperities of the road will contribute to grip through hysteresis, but dis-allow full adhesive contact. However, as more cars pass over the same piece of road, warm rubber will be worn off the tyre and get stuck in the cavities of the road, as seen in Figure 35. This is known as the track being *rubbered in*, giving rise to a larger effective area of contact and increased adhesive grip (Dunlop, 2010).

Figure 35 – Rubber which is stuck to the road can aid adhesion (Dunlop, 2010)

3.4.3 Fluids

When a fluid such as rainwater lands on the road surface, it stays between the asperities of the road until drained or evaporated.

In dry conditions, (a) of Figure 36, the rubber will wrap around the asperities of the road to maximise the effect of hysteresis and adhesion.

In damp conditions only a small portion of the cavities will be filled with water, removing some of contact area used to create adhesive grip. However, since the larger asperities are responsible for the majority of the hysteretic friction, this component remains relatively unchanged (Haney, 2003).

In the case of standing water (b), the tyre will seal the water in the cavities and eliminate the adhesive grip (Persson, Tartaglino, Albohr, & Tosatti, 2005).

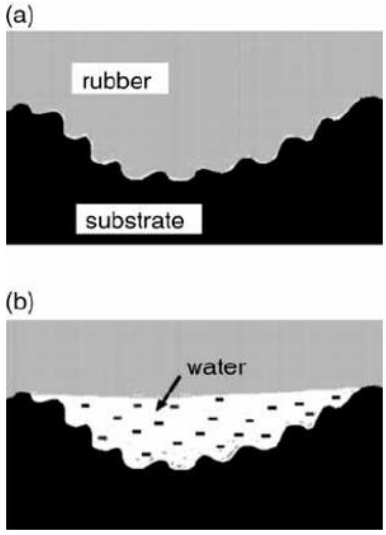

Figure 36 – Water is sealed within cavities (Haney, 2003)

On a normal race track, a certain path will offer the highest average speed over a lap, given a certain car on a dry surface. This is known as the *racing line*, typically derived from maximizing the path radius while still staying between the edges of the track. Over time, frequent driving on the same piece of tarmac will result in the most prominent peaks getting polished, demonstrated as (b) in Figure 37.

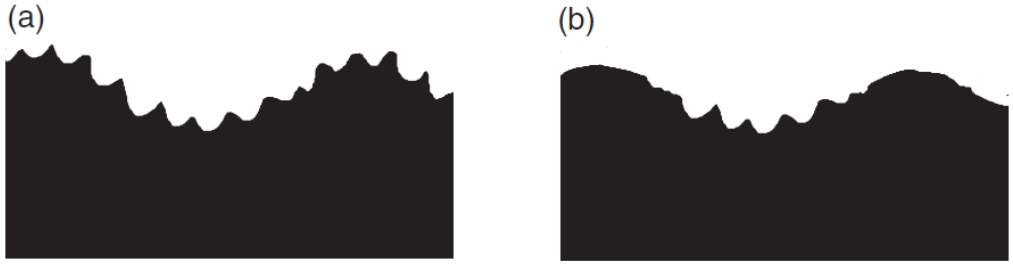

Figure 37 – The racing line gets polished (Haney, 2003)

In the case of a wet track, this would remove some of the asperieties which would aid the generation of hysteretic grip. This is why the racing line may be different in dry and wet conditions (Haney, 2003), adding a track-dependant element to fully modelling the interaction between tyre and track.

3.5 Degradation Phenomena

Depending on the thermal state of the tyre, various degradation phenomena will affect the structure of the rubber. Through the interplay between tread and re-inforcements, the stresses and deformations may cause slow or sudden loss of performance.

There is a temperature range in which the tyre is designed to operate. In this window, wear will take place, but in a manageable way. High stresses outside this window is likely to have critical effects on tyre health, either through graining or blistering.

3.5.1 Graining

In the beginning of a driving session it is common for a tyre to be cold, both on the inside and outside surface. If excessive stress is put into the tyre at this stage, the brittle characteristics of the cold rubber may lead to deformation beyond the point of recovery. These failures are known as graining, resulting in rubber pieces being torn or rolled off the tyre, as seen in Figure 38. This is caused by the local stress exceeding the tensile strength of the rubber, particularily in regions around sharp asperities (Haney, 2003).

Figure 38 – During graining, tyre pieces are being rolled and torn off the tyre

3.5.2 Wear

As the rubber compound is reaching its operating temperature, flexibility will increase. This prevents deformation from tearing of larger rubber pieces and allows the tyre to sustain greater stresses. However, when large forces and high slip velocities are combined, the rubber will experience extreme stress and therefore local temperature peaks around the road asperities. This phenomena is known as *flash temperature* (Persson B. N., 2014), causing the rubber to change in composition and form a thin layer with poor mechanincal properties (Persson, Tartaglino, Albohr, & Tosatti, 2005) which can easily be worn off in a similar fashion to that of graining. Wear rate is therefore commonly assumed to be proportional to the slip power of the contact patch (Knisley, 2002) (Lupker, Cheli, & Braghin, 2004).

With the main cause of wear being high stress concentrations, it can be understood that the wear rate will be higher for tyres with tread blocks compared to that of slick tyres. This since the load will be concentrated around the edges of the blocks, demonstrated in Figure 39, rather than the more even distribution of a slick tyre (Dunlop, 2010).

Figure 39 – Edges of a tread block will experience high stresses (Dunlop, 2010)

3.5.3 Blistering

Upon overheating of the tyre, the rubber enters a state of *reversion*, meaning that it returns to its natural soft state rather than vulcanise towards a more rigid state. If this only occurs on the outer surface, typically when a wheel is locked up during braking, the soft rubber is scraped off. While this may not be critical, it generates *flat-spots* that cause instabilities (Catsburg, 2017), similar to the ones covered in Section 3.4.1.

Overheating of the core and inner surface may lead to separation between tread and its re-inforcements, causing blisters to form and eventually make pieces of rubber break loose from the tyre (Pirelli, 2011). Due to the hard rubber compounds and relatively low operating temperatures, this phenomena is essentially non-existent within touring car racing (Mohlin, 2017).

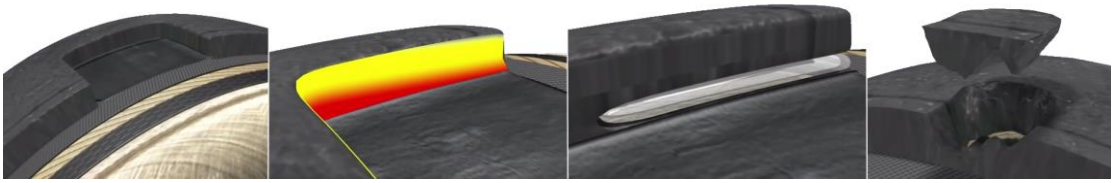

Figure 40 – Blistering is caused by overheating the tyre (Pirelli, 2011)

4 Model

Modelling the performance evolution of a tyre that is operating close to its limit, over a longer period of time, is a complex matter. Its ability to produce grip will be dependant on the thermal and mechanical state, requiring these aspects to be modelled before pursuing the endeavour of taking a physical approach to understanding the workings of tyre and road interface.

As the primary method of evalutation has been set to subjective assessment, the key implementation of the model will be in a motion-based driving simulator. The vehicle model of the system used by Cyan Racing is based on Simulink (MathWorks, R2015b), allowing MATLAB (MathWorks, R2015b) code to be run as modules within the simulation. To ensure high levels of realism the model runs at 1000 Hz, requiring powerful computational hardware and sufficiently low modelling complexity to not exceed 1 ms per cycle.

4.1 Overview

The current models available at Cyan Racing offer good accuracy in terms of describing the relation between a slip input and the corresponding road-plane forces that arise, given a certain vertical load and wheel alignment. However, it is carried out without accounting for thermal influences, resulting in a lack of existing thermodynamic models for the unsprung components. To model the evolution of grip and stiffness, calculations for heating and cooling of the tyre must first be carried out.

In a motorsport application, the aggressive use of camber to enhance cornering performance will result in a highly uneven lateral load distribution. This means that each segment of the tyre will evolve differently, causing the available performance to be dependant on both thermal state and alignment between tyre and road.

4.1.1 Structure

The evolution model should be integrated by scaling the calculated tyre force based on the current and previous vehicle states. In a driving simulator, the user input is fed through component models and equations of motion, giving rise to tyre forces that will affect the vehicle path. Here the calculated forces will be intercepted before affecting the chassis, scaled according to the preferences of the evolution model and parsed along their original calculation path. This approach has been chosen to ensure that the evolution model can be used with different tyre models.

The schematics of this data flow is demonstrated in Figure 41. The vehicle model is providing the tyre model with information about the loading and alignment of the wheel in relation to the road, but also the amount of lateral and longitudinal slippage that is taking place. This results in lateral and longitudinal road-plane forces that are to be individually scaled as in Equation (4.1) by one factor P per direction, P_x and P_y.

The scaled forces will then be used to calculate chassis movements, but also to update scaling for the next time step. Each factor will relate to different physical phenomena.

- Abrasion – Section 3.2.1 & 3.5.2
- Inflation – Section 3.1.6 & 3.2.2
- Vulcanisation – Section 3.1.3 & 3.3.1
- Heating – Section 3.1.3 & 3.3.1
- Contamination – Section 3.4

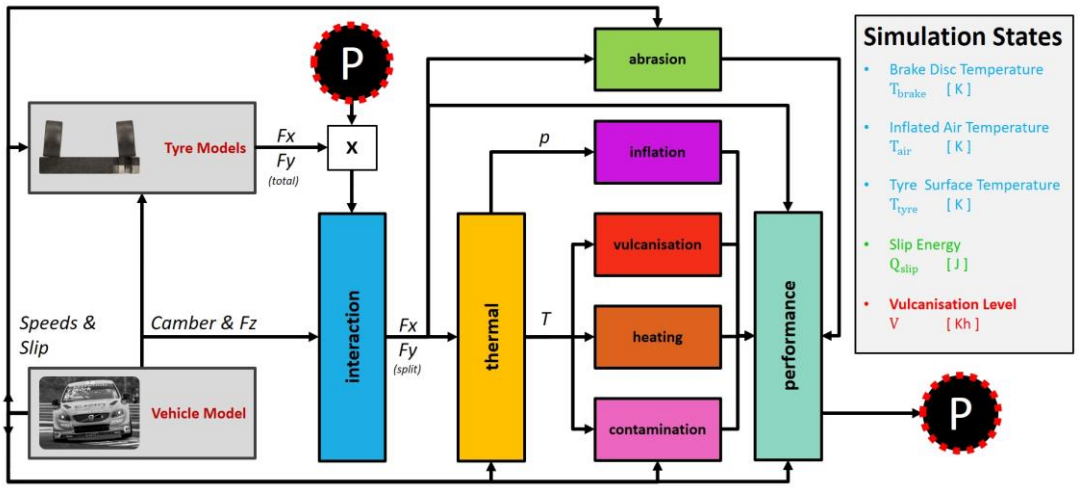

Figure 41 – Interaction between the different models, detailed in Appendix A

$$\sum F_{x_{split}} = F_{x_{total}} * P_x \quad , \quad \sum F_{y_{split}} = F_{y_{total}} * P_y \qquad (4.1)$$

In order to calculate how stress levels will vary over the contact patch, a surface interaction model covered in Section 4.2 will estimate how much of the total tyre road-plane forces that is being produced by each segment. This combined with previously extracted speed and slippage data is then used to calculate thermal exchanges between unsprung components. This is covered in Section 4.3 and allows for estimation of tyre temperatures for each segment, but also inflation pressure.

Given the states calculated in previous steps, five performance altering phenomena are modelled. They either affect the cornering stiffness or the peak grip, in a reversible or irreversible manner as demonstrated in Figure 42 and elaborated in Section 4.4.

All of the mentioned submodels shown in Appendix A are then packaged inside the simulation block shown in Figure 43 with a limited set of inputs and outputs. The ports marked *control*, *param* and *debug* are used to activate the model, feed constants and store simulated values.

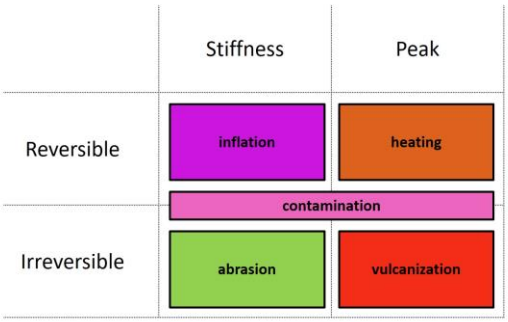

Figure 42 – Five evolution phenomena

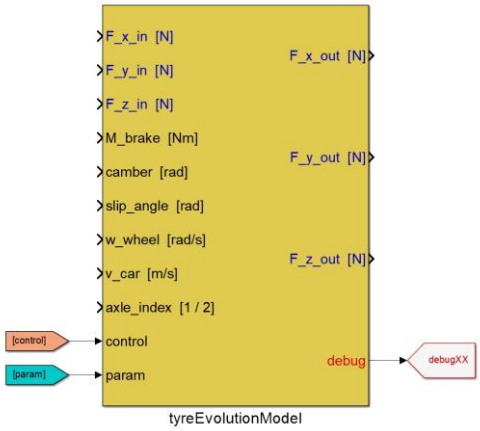

Figure 43 – The model ports

4.1.2 Parameterisation

In order to run the model, several physical phenomena have been analysed to extract correlations that could be used in a simulation environment. The available data sets contain races from the 2016 World Touring Car Championship and isolated tyre tests.

The surface interaction and thermodynamic models are necessary and their accuracy will influence how the simulated tyres evolve, but these models will not be given excessive attention as they are not core parts of the thesis.

The required thermal exchanges have been modelled based on analysing the temperature fluctuations of unsprung components and correlating them to external phenomena. Parameters for stiffness alteration have been extracted from tyre testing data, while changes in peak performance have been identified as trends in race run data. Several relations, such as performance drop per temperature deviation or tyre heating per slip power, are assumed to be linear to minimise the amount of variables required for tuning.

4.2 Surface Interaction

Interaction between car and road will lead to an uneven loading of the contact patch, resulting in varying performance evolution for different parts of the tyre. It is therefore important to model this aspect in order for setup changes to affect the dynamics in realistic manner. Due to the complex nature of this phenomena, a simplified approach has been utilised to reduce impact on the core topic.

4.2.1 Pneumatic Scrub

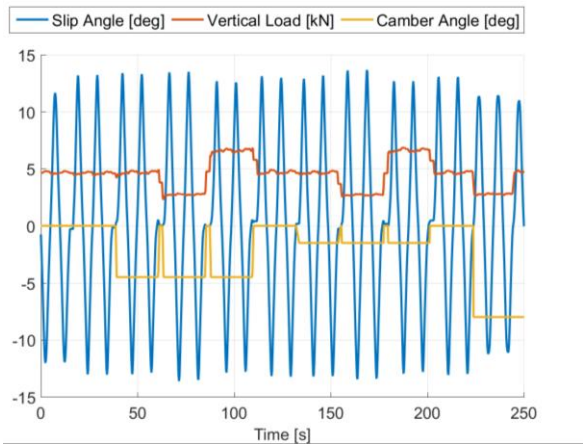

Figure 44 – Tyre testing procedure

The assumption behind the surface interaction model is that centre of pressure will migrate sideways in proportion to the utilised lateral friction, but be counteracted by the effective camber angle of the wheel. Parameterisation of this is done by analysing tyre test data where the vertical load, camber and slip angle are varied, as shown in Figure 44.

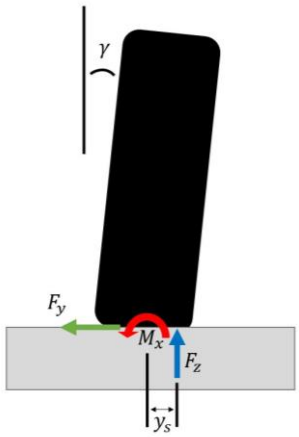

Figure 45 – The vertical force offset

This give rise to a lateral force F_y, but also an overturning moment M_x which is induced by the resulting vertical force F_z being applied at an offset y_s, known as *pneumatic scrub*, from the tyre centreline. This is shown in Figure 45, with the relation between M_x and F_z calculated according to Equation (4.2).

$$y_s = \frac{M_x}{F_z} \qquad (4.2)$$

Parametersation of the surface interaction model has therefore been done by first isolating data with an insignificantly small slip angle and side force, but where a significant amount of camber is being applied. This to identify y_{camber} which describes the centre of pressure lateral migration per inclination of the wheel. The opposite criteria is then used to identify $y_{friction}$ where the amount of migration is compared to the utilised lateral friction μ_y, described by Equation (4.3).

$$y_s = \mu_y \cdot y_{friction} + \gamma \cdot y_{camber} \quad , \quad \mu_y = \frac{F_y}{F_z} \qquad (4.3)$$

4.2.2 Load Distribution

The pressure profile for a front-view cross-section of the tyre is shown in Figure 46. For the assumed linear distribution, the point of peak surface pressure must have a greater offset y_p to the tyre centreline than that to the centre of pressure y_s, given that the tyre is in full contact with the road, $y_d = 0$. This can be understood as the areas under the pressure profile line must be equal on both sides of the point in which the resultant force is acting.

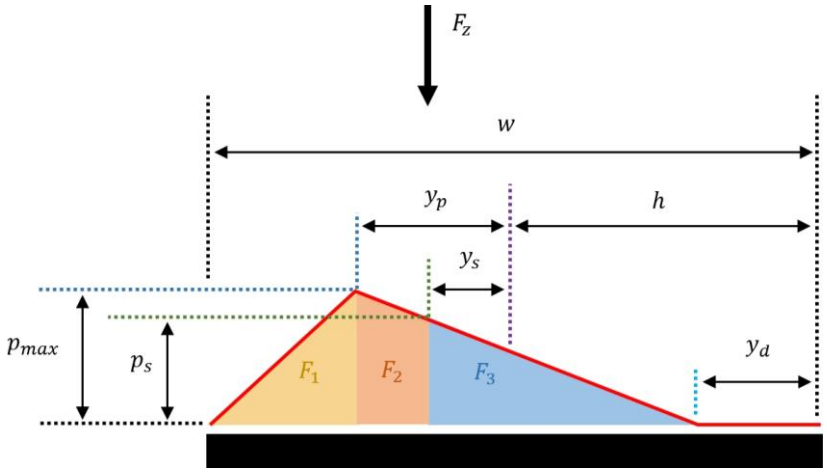

Figure 46 – The pressure profile of a tyre

Knowing the tyre width, total vertical force and simulated centre of pressure migration, we can now derive Equation (4.11) as a general model for locating the point of peak pressure. The tyre can then be split into evenly sized segments and their respective load contribution can be calculated as the area under the pressure profile for that segment. By neglecting the load degressive nature of the rubber, it can further be assumed that the vertical and road-plane forces are split proportionally.

$$h = \frac{w}{2} \tag{4.4}$$

$$p_{max} = \frac{2F_z}{(2h - y_d)} \tag{4.5}$$

$$p_s = \frac{(h - y_d + y_s)}{(h - y_d + y_p)} \cdot p_{max} \tag{4.6}$$

$$F_1 = \frac{(h - y_p)}{2} \cdot p_{max} \tag{4.7}$$

$$F_2 = \frac{(p_{max} + p_s)(y_p - y_s)}{2} \tag{4.8}$$

$$F_3 = \frac{(h - y_d + y_s)}{2} \cdot p_s \tag{4.9}$$

$$F_3 = F_1 + F_2 \tag{4.10}$$

$$y_p = y_s \cdot \frac{(2y_s + 4h)}{(2h - y_d)} + y_d \cdot \frac{(y_d - h - 4y_s)}{(2h - y_d)} \tag{4.11}$$

In the case of large migrations, y_p will be limited to the value of h, requiring $y_d > 0$ in order for the centre of pressure to be in the correct position.

In practical terms, this means that the unloaded side of the tyre will start to lift upon large camber angles without side force or in the case of a large side force without appropriate camber. This is demonstrated in Figure 47.

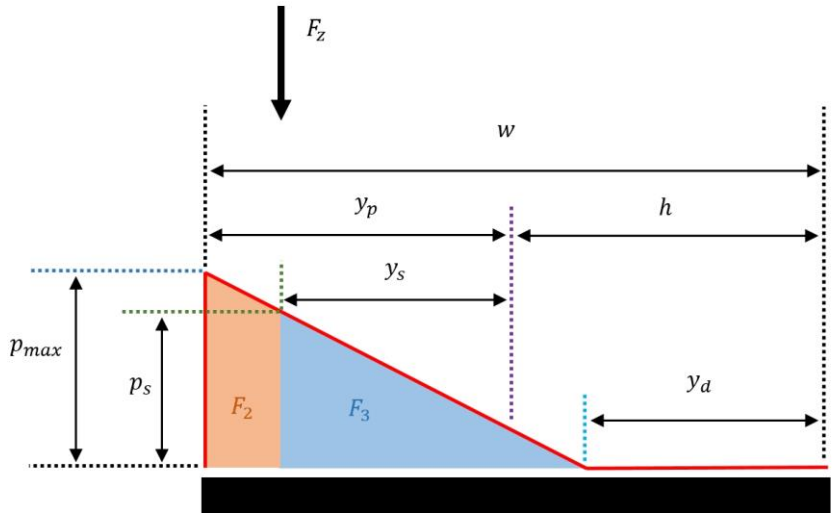

Figure 47 – The peak pressure will be on the edge and the unloaded side will lift

The width of the unloaded segment y_d can be calculated as per Equation (4.16).

$$p_s = \frac{(h-y_d+y_s)}{(2h-y_d)} \cdot p_{max} \quad (4.12)$$

$$F_2 = \frac{(p_{max}+p_s)(h-y_s)}{2} \quad (4.13)$$

$$F_3 = \frac{(h-y_d+y_s)}{2} \cdot p_s \quad (4.14)$$

$$F_3 = F_2 \quad (4.15)$$

$$y_d = 2y_s - \sqrt{2} \cdot (h - y_s) \quad (4.16)$$

4.3 Unsprung Thermodynamics

The intense use of all components in the unsprung assembly is known to generate a large amount of heat. These hot surfaces will then be cooled off due to thermal exchanges between components, but also due to the cooler environment.

As shown in Figure 48 and demonstrated more clearly in Section 5.1.2, the brake disc will get siginificantly hotter than the tyre surface. It can also be seen that during the majority of the session, the inflated air will be hotter than the tyre surface. This confirms the theory (Mohlin, 2017) (Haines, 2011) that brake discs heat the rim, which in turn will heat the inflated air. Unfortunately, no temperature data exist for the rim as it's not a safety critical aspect for the car.

While the tyre surface temperature will have a strong effect on grip and wear resistance, core rubber temperature will affect both the tyres' ability to wrap around road asperities and its hysteretic response to excitation. The hot inflated air will continuously heat the inner tyre surface and thereby prevent the core rubber temperature from dropping, which is one of the reasons behind why it is important to quickly get the brakes up to their nominal operating temperature in the beginning of a session.

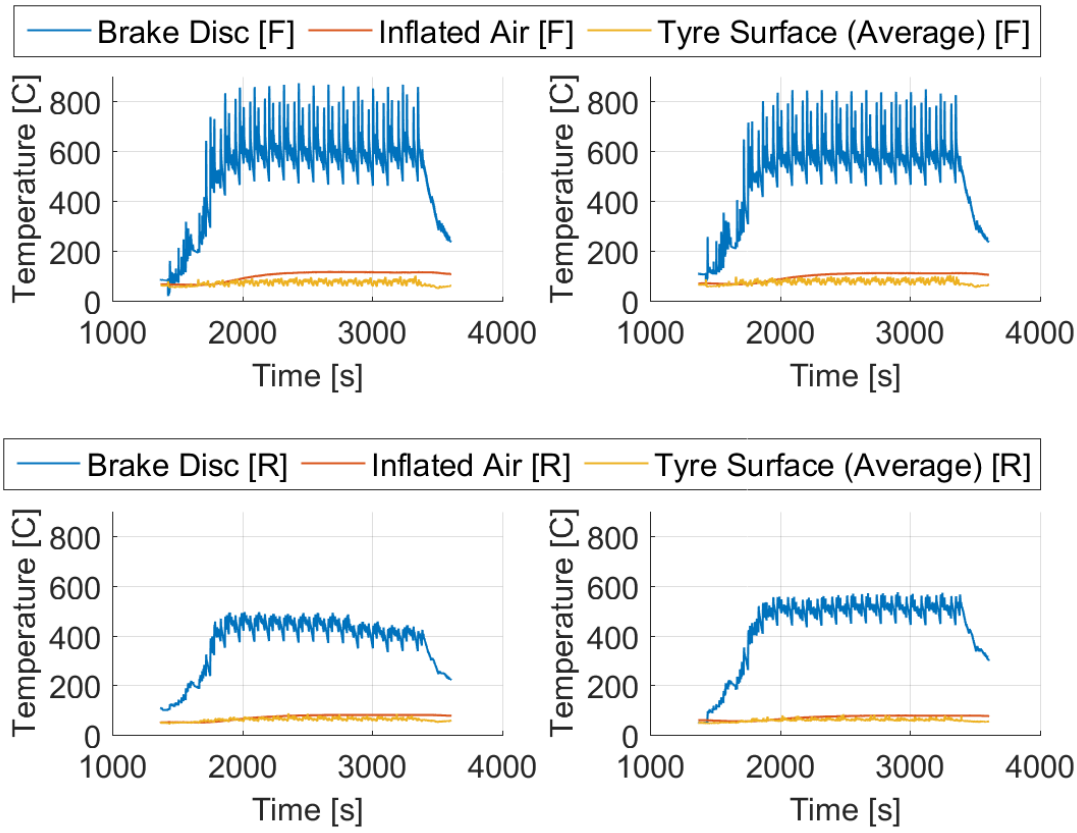

Figure 48 – Temperature measurements of unsprung components

Parameterisation of the thermodynamic model has been simplified by neglecting the fact that a temperature reading only represents the surface, allowing the contained energy Q within a component to be estimated according to Equation (4.17), assuming mass m and specific heat capacity c_p for the different components.

$$Q = c_p \cdot m \cdot T \tag{4.17}$$

The contained energy will then vary over the course of a session. When energy is flowing into the material in the form of heat, the temperature will go up. The opposite is true when energy leaves the material in the form of cooling. To simplify parameterisation, the change of contained energy has been devoted to either heating or cooling, preventing them from occurring simultaneously.

For each component, external heating and cooling phenomena has then been identified, allowing them to be compared to the change of contained energy. Each phenomena is then given fictive scaling factors, h and c, which can be used in the simulation model described through the front-view cross-section of Figure 49. Note that yellow and blue object are mere visualisations of thermal exchanges and not physical objects.

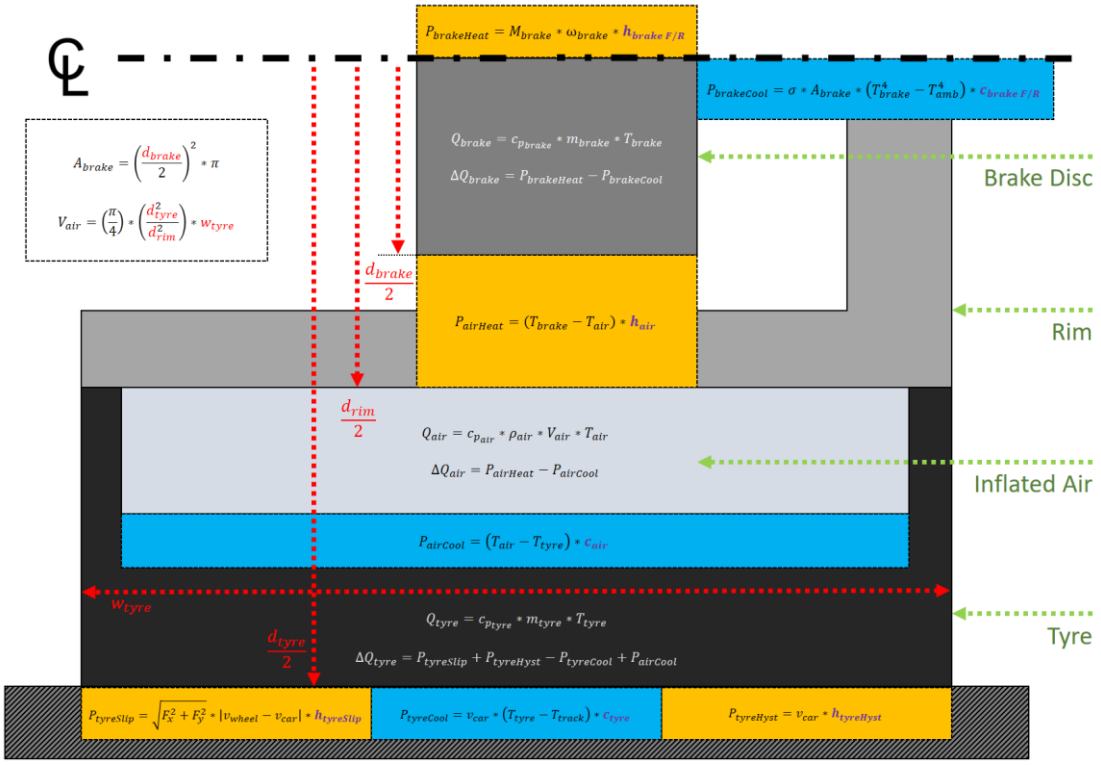

Figure 49 – Cross-section used to demonstrate the thermodynamic model

4.3.1 Brake Disc

The brake discs are made of steel, but with a significaly larger diameter and weight on the front axle to cope with higher stresses. The heating is set as proportional to the braking power of the disc, defined as stopping torque multipled by wheel rotational speed. This is then multiplied by either h_{brakeF} or h_{brakeR} depending on the chosen axle according to Equation (4.18).

$$P_{brakeHeat} = M_{brake} \cdot \omega_{brake} \cdot \boldsymbol{h_{brake\ F/R}} \qquad (4.18)$$

As seen in Figure 50, there is a significant non-linear relation between cooling rate and brake disc temperature. Due to the high temperatures, it has been assumed that the cooling is primarily caused by radiation. The *Stefan-Bolzmann law* has therefore been employed according to Equation (4.19), taking the ambient temperature into account.

$$P_{brakeCool} = \sigma \cdot A_{brake} \cdot (T_{brake}^4 - T_{amb}^4) \cdot \boldsymbol{c_{brake\ F/R}} \qquad (4.19)$$

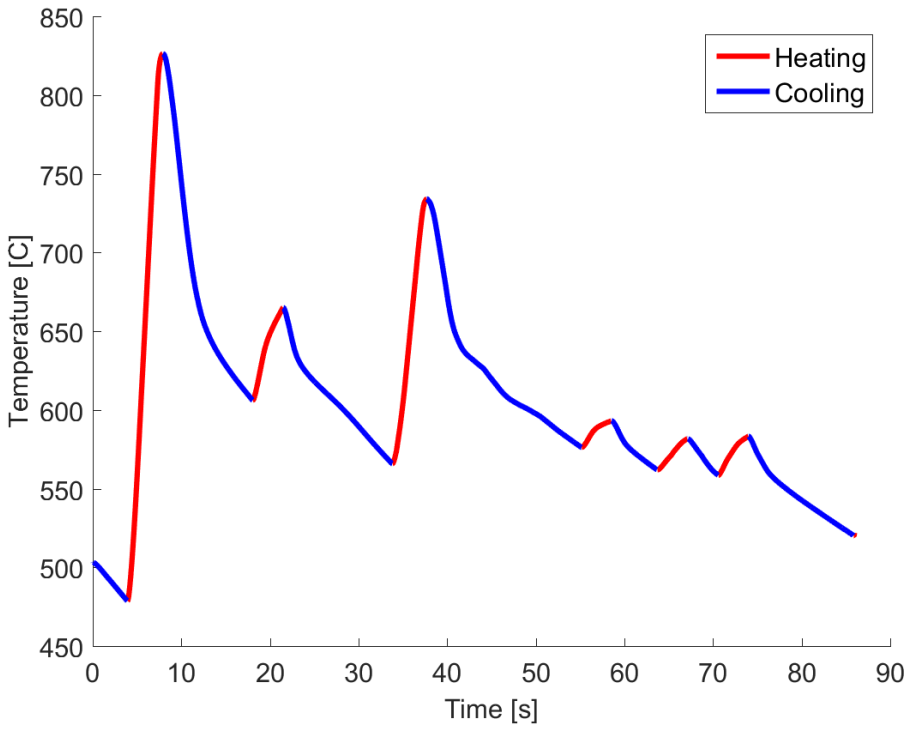

Figure 50 – Brake cooling is not linearly proportional to its temperature

4.3.2 Inflated Air

The heat of the brake disc will be transferred via the rim to the inflated air. However, since no temperature data exist for the rim, it has been discarded in the model. Being a large metal structure which would have to be warmed up before the heat would affect the air, neglecting it will inevitably lead to more rapid heating and cooling. By knowing starting pressure and calculated temperature, the *ideal gas law* can then be used to calculate the current inflation pressure.

The air heating rate is set as proportional to the temperature difference between brake disc and inflated air according to Equation (4.20).

$$P_{airHeat} = (T_{brake} - T_{air}) \cdot \boldsymbol{h_{air}} \qquad (4.20)$$

The energy transfer between inflated air and tyre rubber will then be dependant on which component that is hotter, but be proportional to their temperature difference according to Equation (4.21).

$$P_{airCool} = \left(T_{air} - T_{tyre}\right) \cdot \boldsymbol{c_{air}} \qquad (4.21)$$

4.3.3 Tyre Rubber

The outer rubber layer is assumed to experience four causes of heat transfer.

1. Slippage between tyre and road, proportional to the slip power defined as the relative speed difference in the contact patch multiplied by the resultant force.

$$P_{tyreSlip} = \sqrt{F_x^2 + F_y^2} \cdot |v_{wheel} - v_{car}| \cdot \boldsymbol{h_{tyreSlip}} \qquad (4.22)$$

2. Hysteretic energy dissipation in the rubber, propotional to vehicle speed in order to account for the higher excitation frequency that arise as the car moves faster.

$$P_{tyreHyst} = v_{car} \cdot \boldsymbol{h_{tyreHyst}} \qquad (4.23)$$

3. Heat loss due to contact with cooler road surface. This is assumed to occur at an increased rate for high temperature differences, but also upon speed increase due to the same piece of rubber being presented to the road more frequently.

$$P_{tyreCool} = v_{car} \cdot \left(T_{tyre} - T_{track}\right) \cdot \boldsymbol{c_{tyre}} \qquad (4.24)$$

4. The air contained within the tyre will cause it to either cool down or heat up, assumed proportional to temperature differences according to Equation (4.21).

4.4 Performance Alteration

The evolution of tyre performance is split into five phenomena. They are modelled individually and combined in the last calculation step based on the current slip angle.

To enable smooth independent scaling of stiffness and grip, a model based on the inverse trigonometric function *arctan*, shown as purple in Figure 51, has been derived. By defining transition points for linear range P_{lin} and peak grip P_{peak}, the *arctan* curve has been given a positive offset along the x-axis, shown in blue and Equation (4.25).

$$G_{blue} = -\tan^{-1}\left(\left(|\alpha| - \frac{P_{peak} + P_{lin}}{2}\right) \cdot P_{lin}\right) \qquad (4.25)$$

A normalised version has then mirrored around the y-axis, as per the the turquoise line and Equation (4.26), to use the same scaling for both positive and negative slip inputs.

$$G_{turquoise} = \frac{G_{blue} - min(G_{blue})}{max\left(G_{blue} - min(G_{blue})\right)} \qquad (4.26)$$

The curve is then compressed to match the difference between stiffness and grip scaling and moved along the y-axis to fit the desired level. This is shown in Equation (4.27), accompanied by green and yellow lines for 80% and 120% of grip or stiffness scaling, further explained in Equation (4.28) and (4.29).

$$G_{yellow/green} = \left(G_{turquoise} \cdot (STIFF - GRIP)\right) + GRIP \qquad (4.27)$$

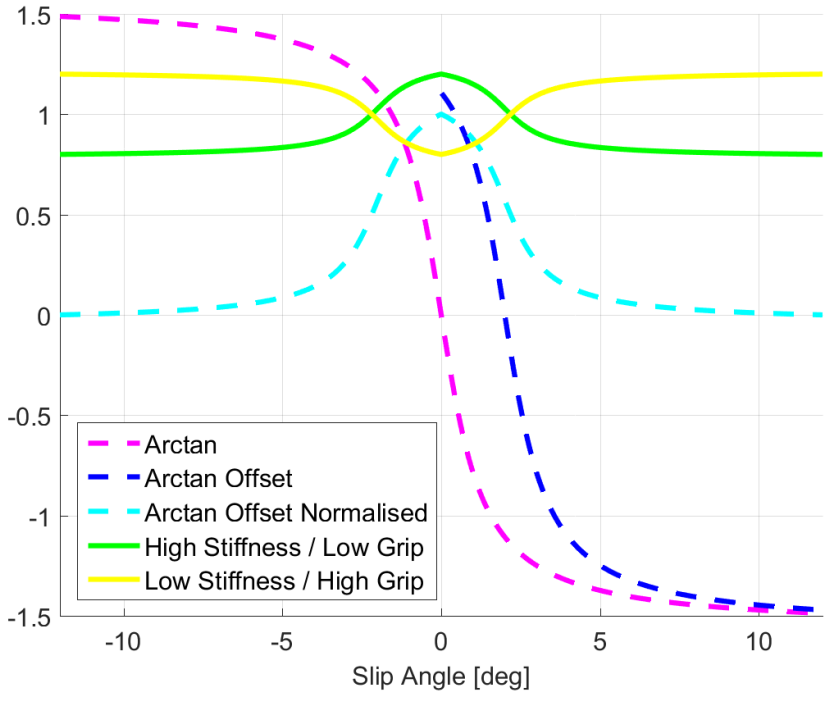

Figure 51 – Transformation of the arctan function

Longitudinal scaling is applied independent of slip ratio due to the lack of data that could support modelling it in a more complex manner, but the lateral force is multiplied by the scaling factor of that particular slip angle. This is demonstrated in Figure 52 for a given slip angle range α and three scaling combinations.

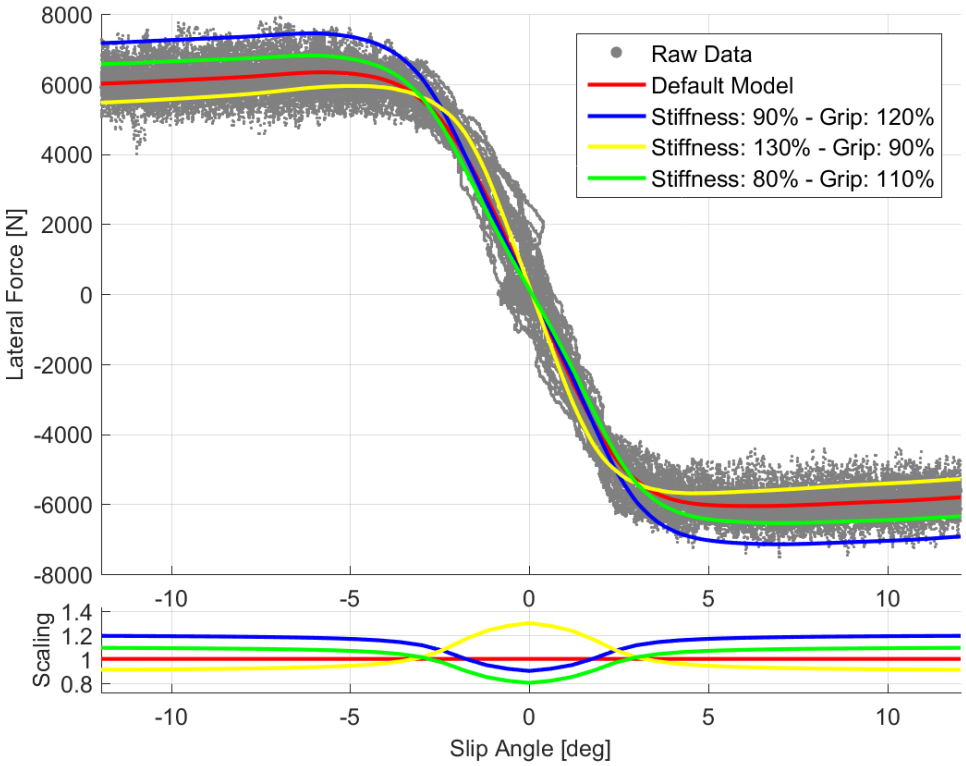

Figure 52 – Scaling of the tyre model

Each of the five submodels will output one scaling factor per direction, denoted as the first letter of the modelled phenomena and the direction in which it should be applied.

A: Abrasion, I: Inflation, V: Vulcanisation, H: Heating and C: Contamination

The merging of these variables is demonstrated in Equation (4.28) to (4.31) with the separation of stiffness and grip scaling shown in Figure 42.

$$STIFF = A_y \cdot I_y \tag{4.28}$$

$$GRIP = V_y \cdot H_y \tag{4.29}$$

$$P_y = f(\alpha, STIFF, GRIP) \cdot C_y \tag{4.30}$$

$$P_x = A_x \cdot I_x \cdot V_x \cdot H_x \cdot C_x \quad , \quad A_x = I_x = 1 \tag{4.31}$$

Since the tyre has been split into several lateral segments which will have experienced varying levels of stress, the scaling factor for any particular phenomena will be different over the width of the contact patch. The scaling factors has therefore been weighed in relation to their portion of the vertical load. Due to the limitations of the project, effects related to contamination are neglected. Parameters C_x and C_y are therefore set to 1.

4.4.1 Abrasion

Abrasive wear is the most commonly discussed form of tyre degradation when it comes to road cars. Due to the tread block design of such tyre, it is commonly assumed that a worn down tyre will get worse at displacing potential water, but also that the tyre become more responsive due to the increase in cornering stiffness that arise thorugh the shearing covered in Section 3.2.1. In a motorsport application, the rubber compound is both harder and significantly thinner in a new condition. Based on measurements acquired on during a race weekend, tyres on the driven axle are rarely worn more than 1 mm over the course of a race that last 10 – 20 laps á ~5 km.

In order to model abrasion, the average wear over the width of the contact patch was measured. This was then assumed to be the thickness of a rubber sheet, representing the rubber material that is to be worn off. Its width is equal to that of the tyre and the length is equal to the tyre circumference, as demonstrated in Figure 53.

Figure 53 – The worn rubber is assumed to start off as a sheet

The slip energy defined in Equation (4.32) was then compared to the volume of the sheet representing worn rubber. This allowed for estimation of abrasive wear in each lateral segment by knowing the total width and number of segments.

$$Q_{slip} = \int P_{slip}(t)\ dt \quad , \quad P_{slip} = \sqrt{F_x^2 + F_y^2} \cdot |v_{wheel} - v_{car}| \qquad (4.32)$$

By comparing isolated tyre test data from new and used states, a minor difference in stiffness was observed as per Figure 54.

To allow for examination of this trend, the stiffness was set to linearly increase by a certain amount per unit of tread wear. The parameters associated with the model are shown in Table 2.

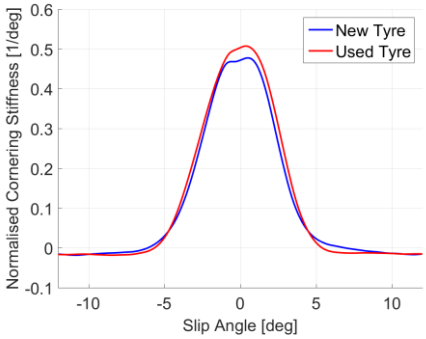

Figure 54 – Normalised cornering stiffness for new vs 0.75 mm worn tyres

Table 2 – Parameters for abrasion model

Parameter	Type	Unit	Description
P_{slip}	Input	W	Slip power of contact patch
A_{wear}	Constant	mm^3 / J	Rubber volume wear rate
A_{cs}	Constant	% / mm	Cornering stiffness increment factor
A_x	Output	-	Longitudinal scaling
A_y	Output	-	Cornering stiffness scaling
A	Output	mm	Rubber wear amount

4.4.2 Inflation

As heat starts to affect the inflated air, the pressure will rise. This leads to an increased tyre stiffness, both in lateral and vertical direction. As per Figure 55, the pressure will have a smaller effect on cornering stiffness compared to vertical stiffness. It can be argued that this is due to the structural sidewall design found in these tyres.

An uneven increase of vertical stiffness between front and rear axle would lead to a change in overall yaw balance, but this has been neglected due to the added complexity of integrating such aspects into the existing vehicle model. The change of pressure is provided by the thermodynamics model. Based on two separate scaling factors, the change of stiffness can then be calculated using Table 3.

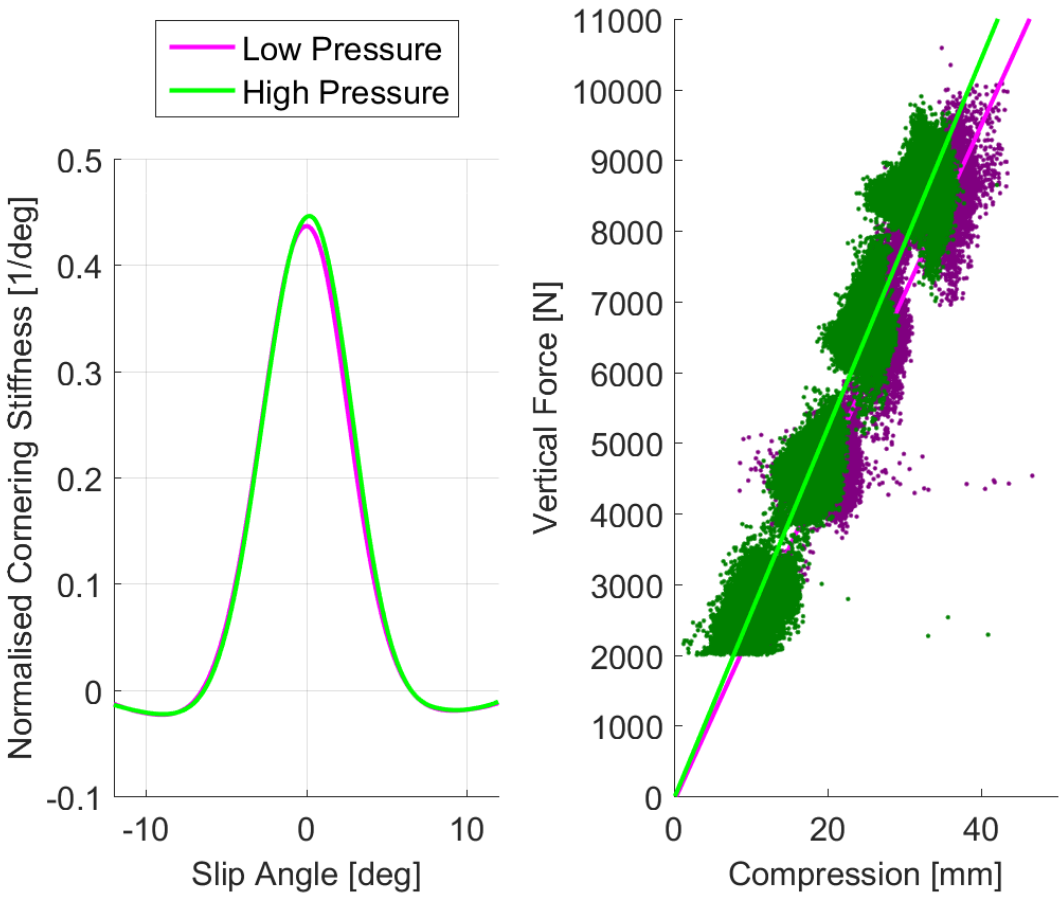

Figure 55 – Stiffness for tyres pressurised to 1.9 vs 2.1 bar

Table 3 – Parameters for inflation model

Parameter	Type	Unit	Description
dp_{air}	Input	bar	Pressure change since start
I_{cs}	Constant	% / bar	Cornering stiffness increment factor
I_{vs}	Constant	% / bar	Vertical stiffness increment factor
I_x	Output	-	Longitudinal scaling
I_y	Output	-	Cornering stiffness scaling
I_z	Output	-	Vertical stiffness scaling

4.4.3 Vulcanisation

When the tyre is excerted to intense stress, the heat generation and mechanical working will be similar to that experienced during the vulcanisation phase of manufacturing. Racing tyres are not fully vulcanised during manufacturing and will therefore be semi-stable when they are new (Haney, 2003). This allows for further curing before the damping that offers hysteretic grip-generation goes away.

Information regarding vulcanisation of this particular compound was not available. However, the essence of this submodel is to penalise operation when the rubber core is at a high temperature and disallow recovery of lost performance. Core temperature was defined as the average of tyre surface and inflated air, with vulcanisation being set to its time integral according to Equation (4.33). Note that it should only be used for vulcanisation that occurs as a result of using the tyre.

$$V = \int \frac{T_{air}(t) + T_{tyre}(t)}{2} dt \qquad (4.33)$$

Accelerations in both lateral and longitudinal directions were then normalised over the course of a session so that performance loss could be defined as inability for the car to reproduce its peak accelerations. This, in relation to vulcanisation for the front tyres, is demonstrated in Figure 56. Model parameters are found in Table 4.

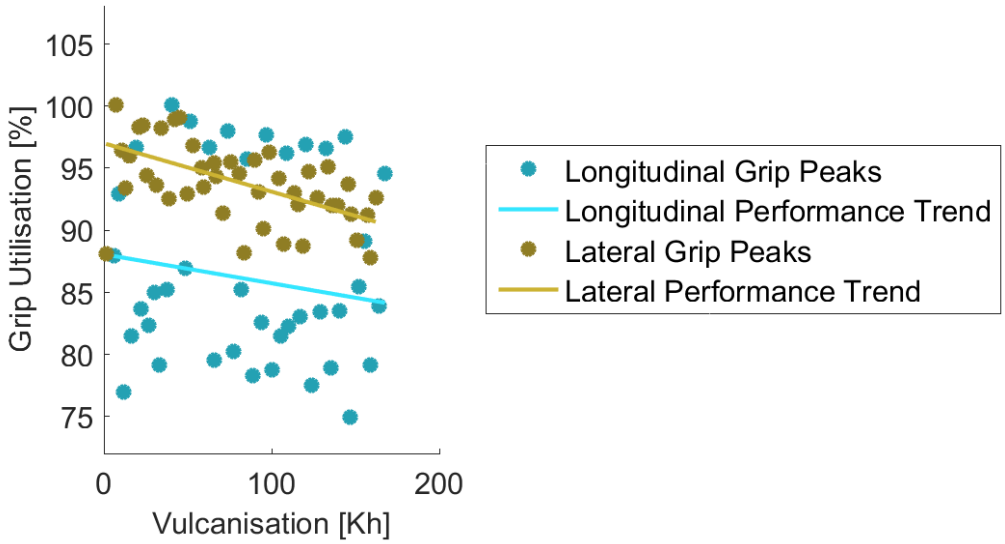

Figure 56 – The grip will decay over the course of a race

Table 4 – Parameters for vulcanisation model

Parameter	Type	Unit	Description
T_{air}	Input	C	Inflated air temperature
T_{tyre}	Input	C	Tyre surface temperature
V_{long}	Constant	% / Kh	Longitudinal grip scaling factor
V_{lat}	Constant	% / Kh	Lateral grip scaling factor
V_x	Output	-	Longitudinal grip scaling
V_y	Output	-	Lateral grip scaling
V	Output	Kh	Vulcanisation level

4.4.4 Heating

For a given excitation frequency of a rubber material, a certain temperature will offer maximum hysteresis. Operating outside this point should therefore bring lower grip.

The temperature range of the tyre surface will vary with track temperature. This results in that modelling a heating penalty based on the absolute temperature of the tyre surface would disallow good performance if the track temperature of the simulation is drastically changed. To compensate for this, data sets from both isolated tyre tests and driving sessions with the real car were analysed.

As per Figure 57, it was observed that the peak friction utilisation was accomplished at a similar level above track temperature for both cold and hot weather driving, but also in the case of a tyre rig test. It was therefore decided that the model was to apply a linearly increasing penalty as the absolute temperature gap between tyre and road move away from the optimum point, using Equation (4.34) and parameters from Table 5.

$$H_x = H_y = 1 - \left| \left| T_{tyre} - T_{track} \right| - H_{opt} \right| \cdot \frac{H_{xy}}{100} \qquad (4.34)$$

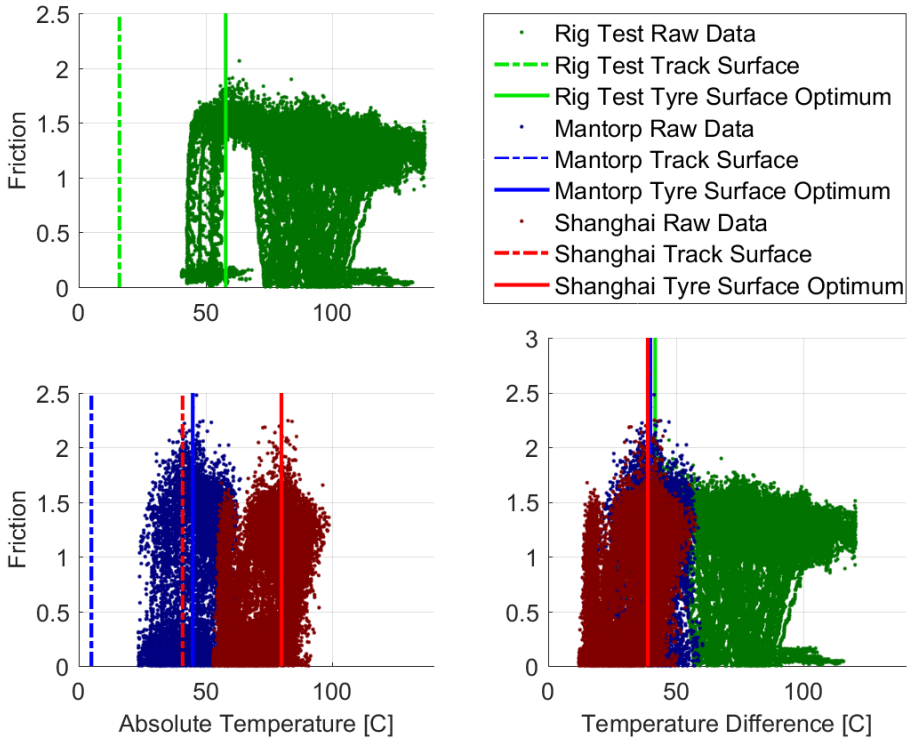

Figure 57 – Temperature difference between track and tyre

Table 5 – Parameters for heating model

Parameter	Type	Unit	Description
T_{tyre}	Input	C	Tyre surface temperature
H_{opt}	Constant	K	Optimal temperature difference
H_{xy}	Constant	% / K	Grip scaling factor
H_x	Output	-	Longitudinal grip scaling
H_y	Output	-	Lateral grip scaling

5 Results

The models were developed by feeding them with logged data from the car or test rig and checking their output. This allowed for an effective development process and the time spent allocating the driving simulator could then be used for final implementation and tuning of parameters. The primary method of validation was subjective assessment, so to ensure that the driver would be able to provide accurate descriptions of the effects generated by the evolution model, variables were changed one at the time.

5.1 Data Playback

Stored logdata was fed thorugh the simulation model to validate its output. However, due to the inability to measure everything on a real car, it lacks information about wheel alignment and load. Validation of reponse to camber and lateral slip was therefore carried out with data from isolated tyre tests, while logged vehicle data such as speed and acceleration were used in conjunction with a quasistatic load estimation to validate thermodynamic model response, here in the case of even contact patch loading.

5.1.1 Surface Interaction

A simulated overturning moment can be compared to its measured counterpart by utilising Equation (5.1). The result can be found in Figure 58 and it can be seen that the model lack accuracy for $F_z > 5000\,N$ or $\gamma < -5\,deg$. This is within the operating range of the outer front tyre upon braking into a turn, resulting in a possible exaggeration of shoulder loading in that particular case.

$$M_{x_{simulated}} = F_z \cdot \left(\mu_y \cdot y_{friction} + \gamma \cdot y_{camber} \right) \qquad (5.1)$$

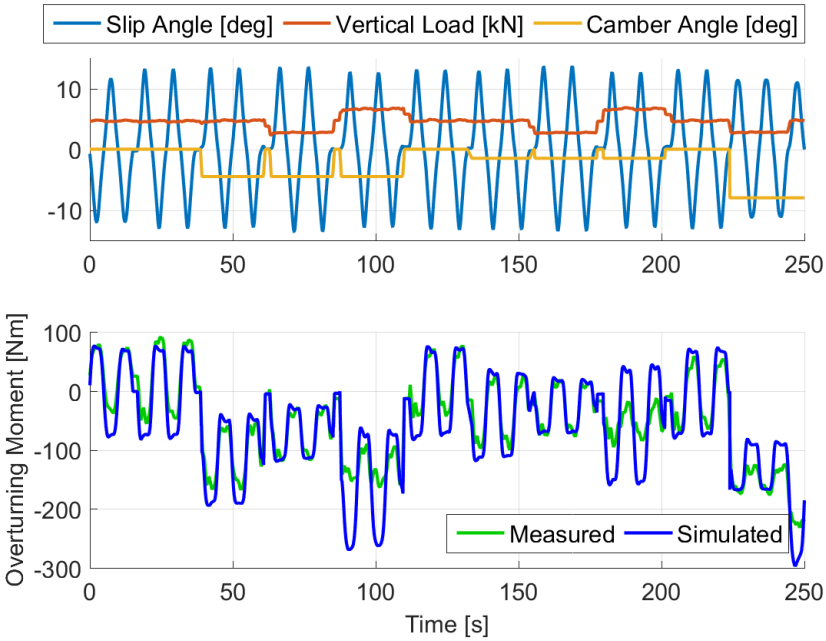

Figure 58 – Comparison of simulated and measured overturning moment

5.1.2 Unsprung Thermodynamics

As the logged data include temperatures, the simulated values can be directly compared to their measured counterparts. Figure 59 shows brake disc temperature over the course of a race, while Figure 60 is highlighting details during a selected portion.

The heating and cooling is controlled by adjusting $h_{brakeF/R}$ and $c_{brakeF/R}$, but it can be seen the discs are generally being simulated as too cold on the rear axle. However, with the inevitable inaccuracies of the quasistatic load estimation used to predict the forces that drive the thermodynamic model, no extensive effort was put into tuning of parameters for the playback environment. It can also be seen that simulated front brake discs reach nominal operating temperature too quickly, but general trends of heating and cooling are captured during the rest of the session.

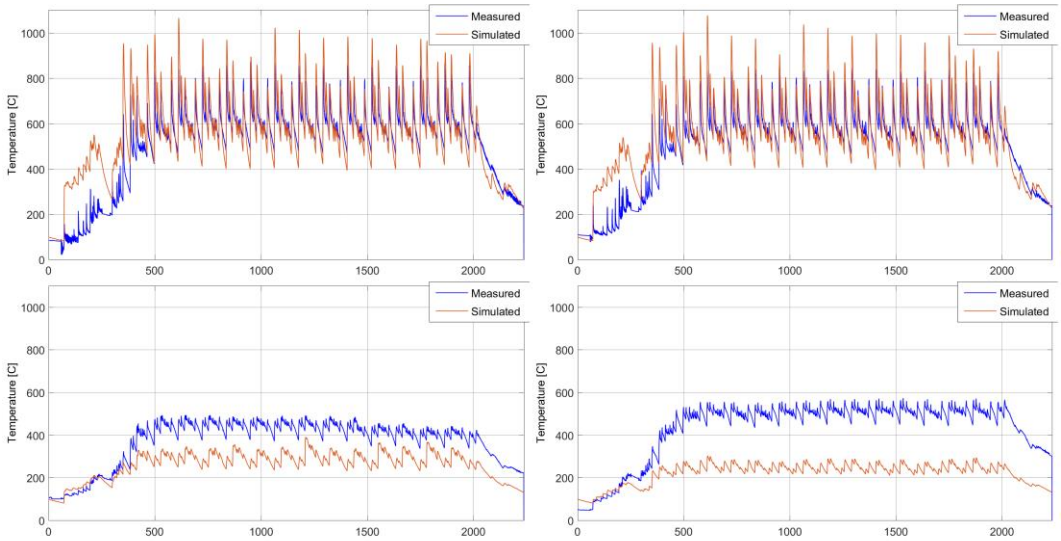

Figure 59 – Full comparison of brake disc temperature

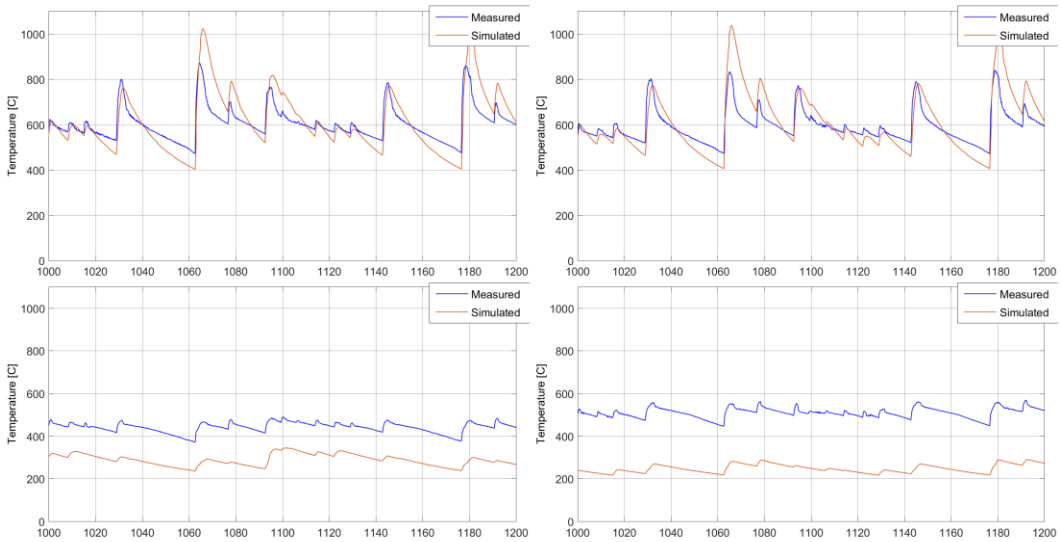

Figure 60 – Partial comparison of brake disc temperature

Figure 61 shows how the inflated air change in temperature over the course of a race. It can be seen that the rate of heating, but also nominal level is modelled with relatively good accuracy. However, the lack of a thermal inertia in the form of a simulated rim is causing the air to both heat up and cool down too early.

Figure 62 shows the change of pressure according to the *ideal gas law*. The pressure change is significantly greater in the real context compared to its simulated counterpart. It has been assumed that this is due to gas being released from the tyre as it is being stressed at high temperatures, but the model still captures general trends and can be adjusted using h_{air} and c_{air}.

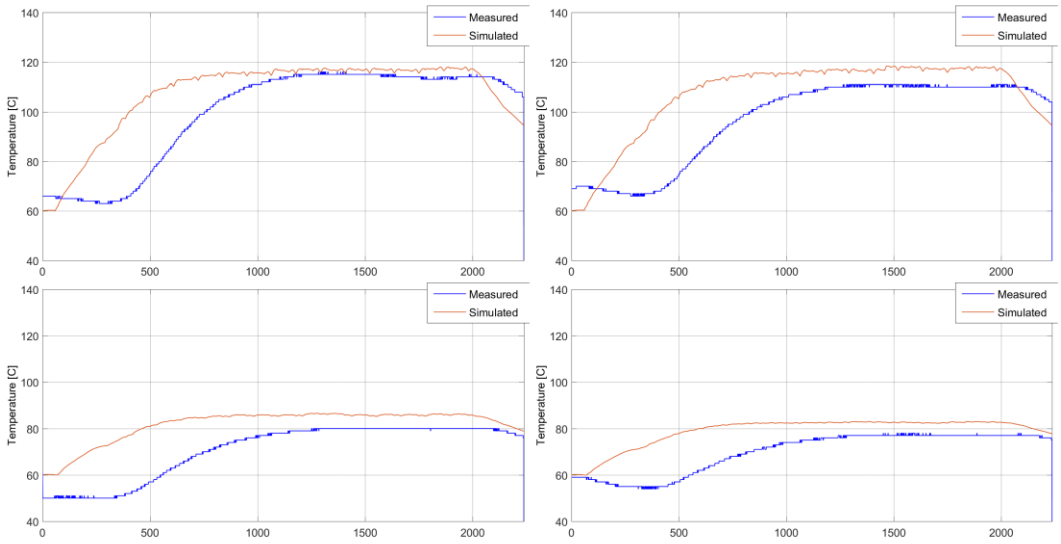

Figure 61 – Full comparison of inflated air temperature

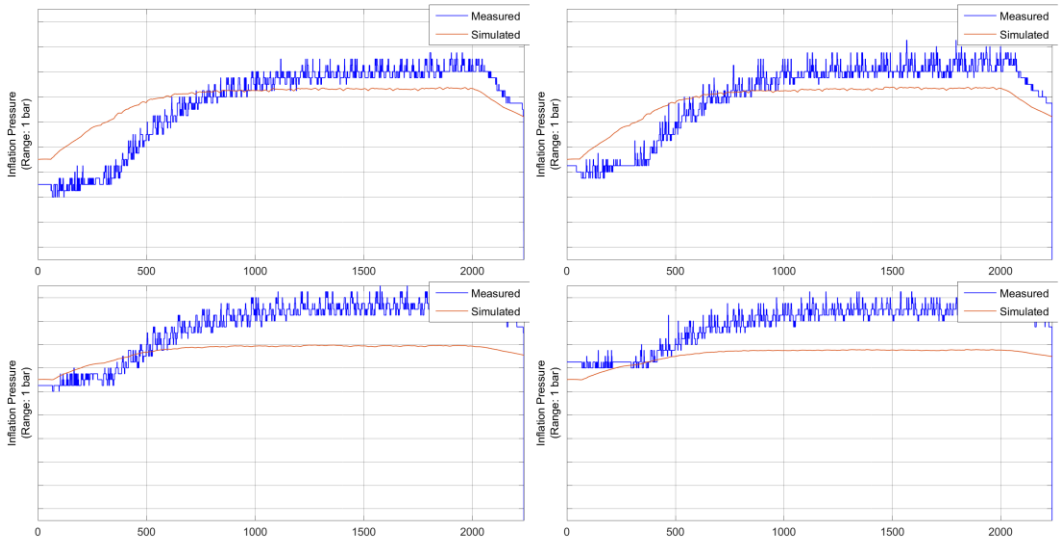

Figure 62 – Full comparison of inflated air pressure

Figure 64 shows how the simulated average tyre surface temperature is reaching nominal temperatures faster than in the real car. It should be noted that the temperature is measured on the part of the surface that is facing forwards. The simulation is assuming the same temperature all the way around for a given lateral tyre segment and that heat transfer takes place in the contact patch. This will inevitably fail to capture aspects such as cooling induced by surrounding air; an effect which may partially explain why sensors are reading low temperatures during the slow warmup laps, seen in Figure 63.

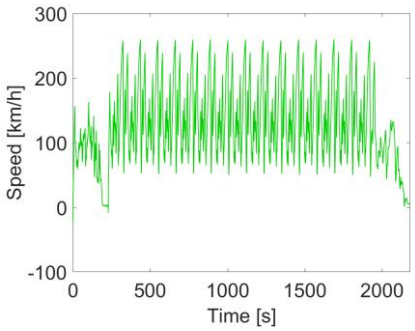

Figure 63 – Speed profile of race in Shanghai

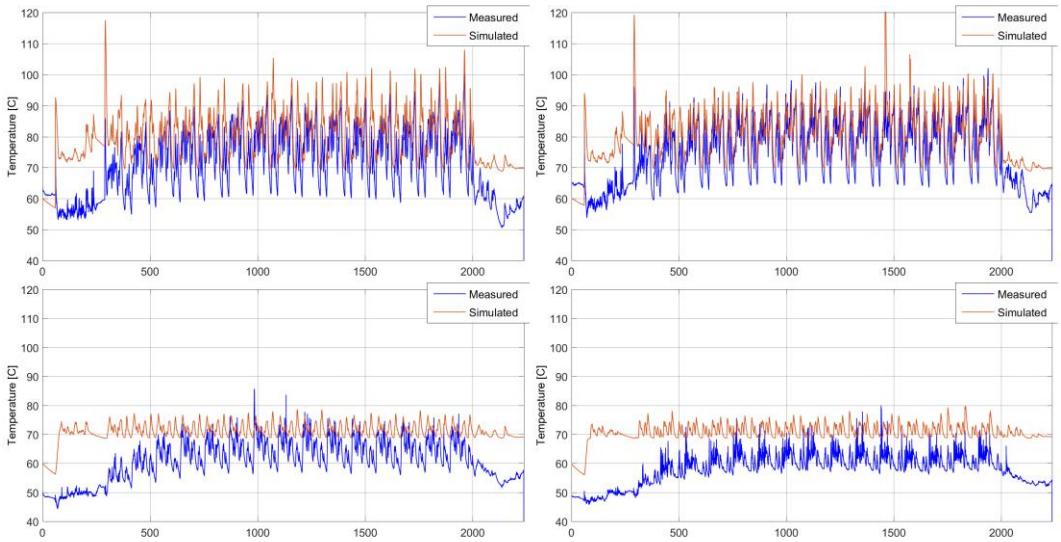

Figure 64 – Full comparison of average tyre surface temperature

Despite this, Figure 65 shows that general trends of heating and cooling are captured.

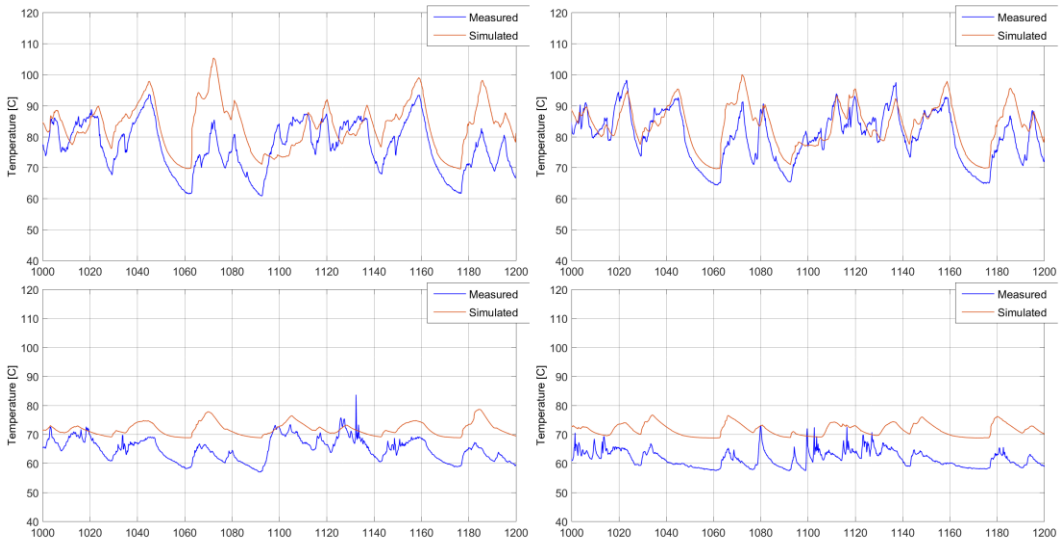

Figure 65 – Partial comparison of average tyre surface temperature

5.2 Driving Simulator

Calculations for load distribution and thermal exchanges were added to the existing vehicle model. Their output was then parsed to the submodels responsible for evolution of tyre performance, allowing them to affect the overall chassis dynamics. The driver then used the simulator shown in Figure 66 to evaluate how the model would respond to parameter changes, according to the test plan of Appendix C.

Figure 66 – Twin Ring Motegi on the driving simulator

5.2.1 Calibration

Since brake torque and tyre forces were approximated when the thermodynamic model was run in a playback environment using the code of Appendix B, a new calibration was carried out. No measured data for load distribution in a real context was available, but the temperature simulations were compared to a similar case from the real car. This by analysing the signal content through histograms and accompanying dashed lines for average temperatures. Extensive effort could be invested in tuning all nine heating and cooling parameters to reach better correlation. However, to better utilise the time allocated in the simulator facility, focus was given to parameters related to tyre performance.

The simulated brake discs still had the same issue of reaching too high temperatures, but also cooling down more than in the real car. More tuning would be required to match desired levels, but the error between average temperature levels was typically below 10 % of the entire temperature range, as seen in Figure 67. Since the brake heat would not directly affect the dynamics of the car, further tuning was disregarded.

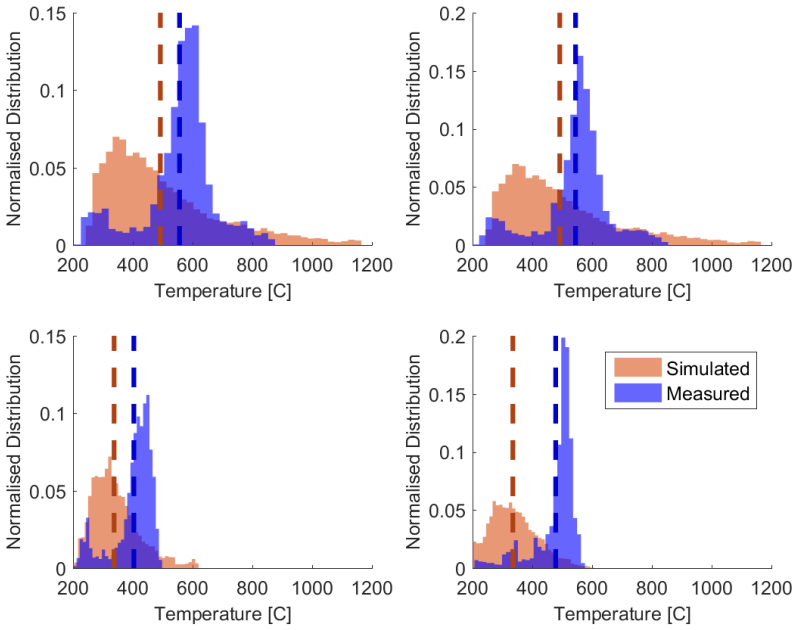

Figure 67 – Signal content of brake disc temperature

Temperature of the inflated air will affect grip through vulcanisation, but also stiffness by changing the inflation pressure. Model parameters were therefore tuned so that the average temperature would be similar to reality, resulting in errors of around 10 ℃ on the rear axle, but only small errors on the front axle, as seen in Figure 68.

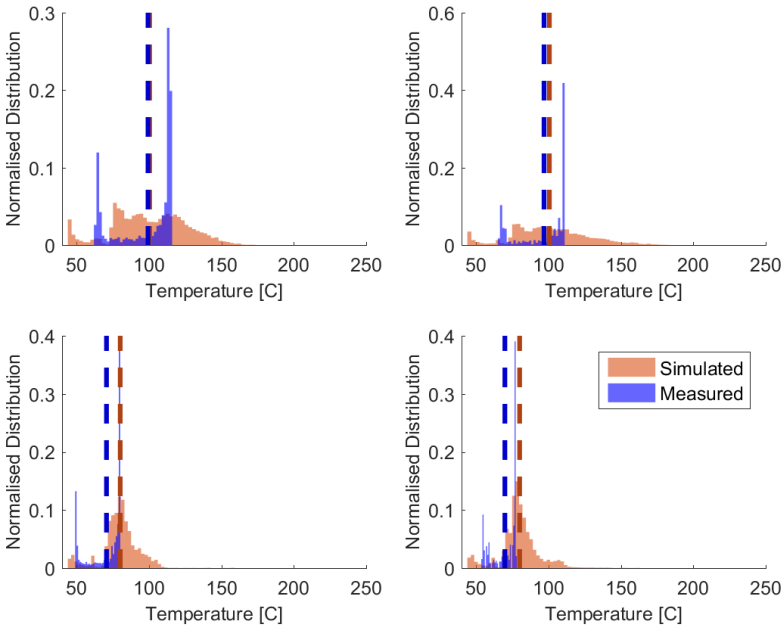

Figure 68 – Signal content of inflated air temperature

Figure 69 shows how the lack of a modelled rim results in temperature fluctuations which do not exist in the real car. The nominal error between measured and average simulated temperature during normal operation is between 2 and 20 ℃, but it should also be noted that the lack of shielding will make the simulated air heat up too quickly.

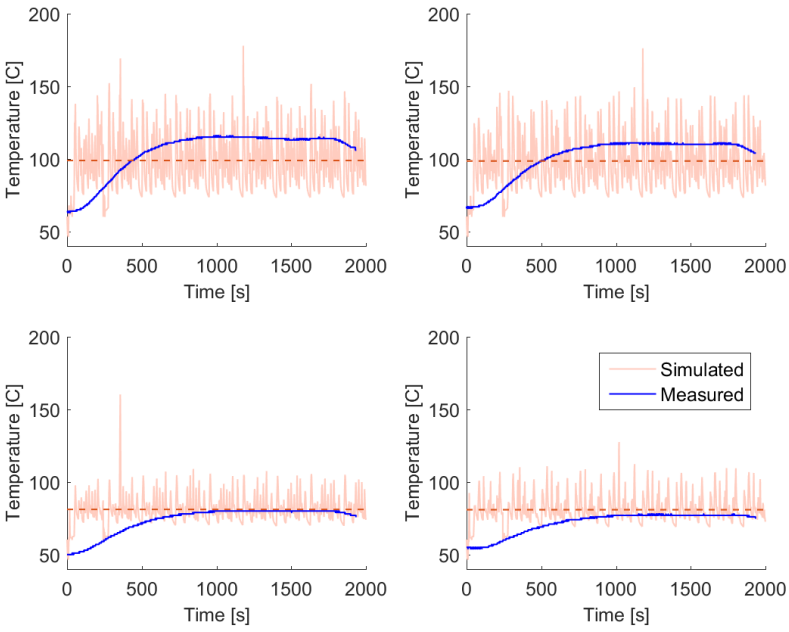

Figure 69 – Variations of air temperature

The simulated tyre surface was running slightly hotter than the measured counterpart, but with the typical error between the average of each signal below 10 °C.

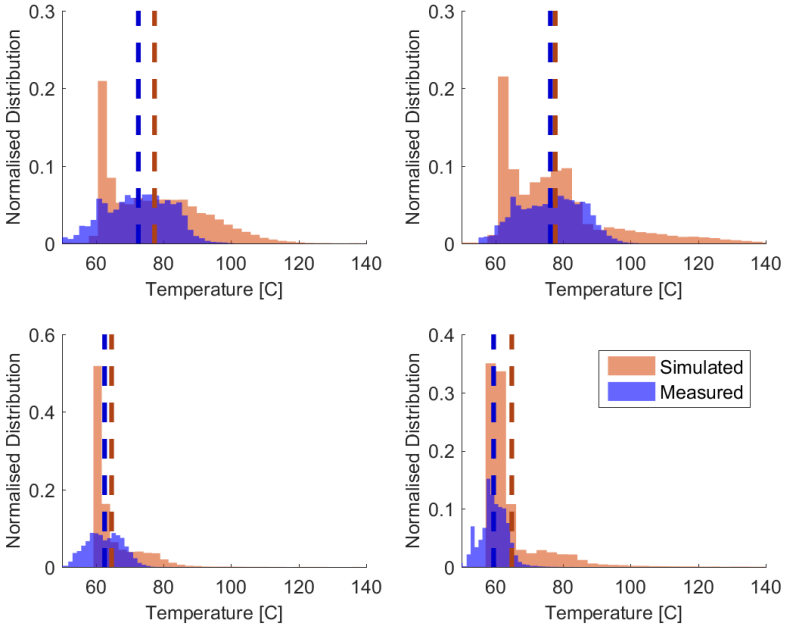

Figure 70 – Signal content of tyre surface temperature

5.2.2 Longitudinal Grip

The performance loss in the longitudinal direction should be less noticeable compared to the lateral loss of performance (Catsburg, 2017) and there was an indication of this being supported by logged vehicle data, as shown in Figure 56. The forces involved in braking manoeuvres are significantly greater than those of propulsion, leading to that the critical stage where this aspect will be subjectively judged is upon heavy braking into a turn.

The scaling of longitudinal forces will only be influenced by the reversible heating penalty or the irreversible output of the vulcanisation model. These two aspects where therefore analysed individually.

The tyres will reach temperatures of around 100 °C during heavy braking when the track temperature is around 35 °C. With the optimal temperature gap presented in Section 4.4.4, this should lead to overheating and therefore grip loss during this phase. The optimal gap was then increased in steps up to the point where those high temperatures would be the ideal point of operation.

Figure 71 shows extremities of the tested cases and their average scaling on front axle. It can be seen that overheating of the tyres is causing a 5 to 10 % grip loss during late stages of corner entry in the normal case, particularily when combined with steering.

As the optimal gap between track and tyre temperature was increased, the tyres would typically be too cold, but get better performance as the car approach the middle point of the corner.

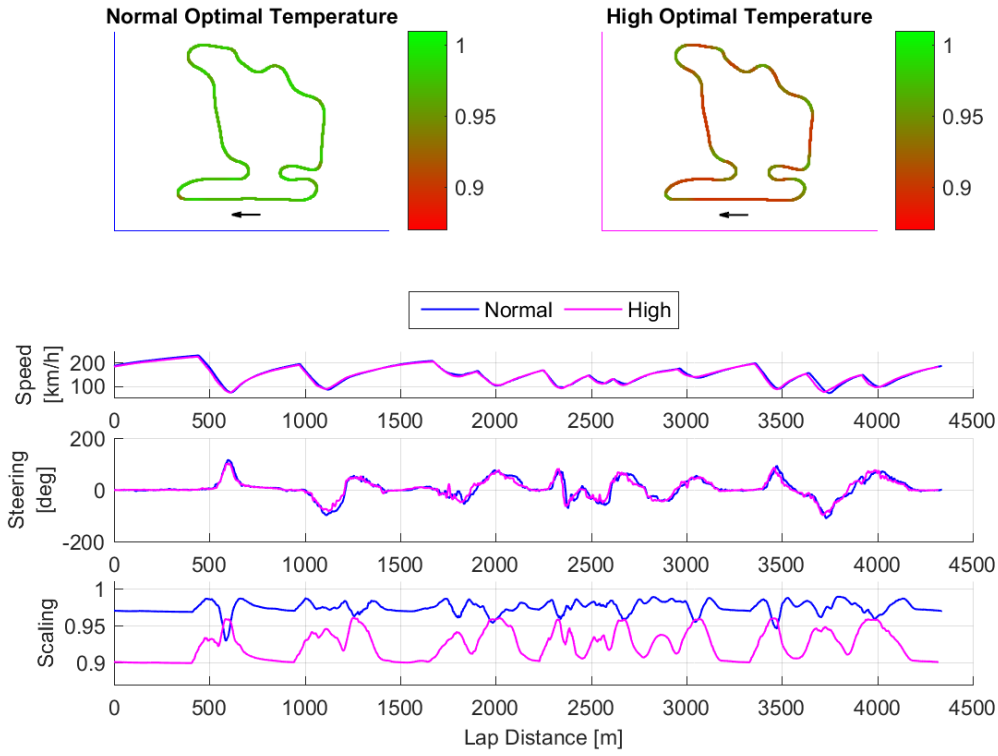

Figure 71 – Optimal temperature variations

The latter case proved to offer unrealistically good corner entry behaviour, but also lack of traction on corner exit which was particularily unrealistic on new tyres. However, it was noted that it's important to reach good entry behaviour before tuning the response during exit. This since a suboptimal entry will compromise the racing line and cause instabilities that end up affecting feedback quality related to the later parts of the corner.

The macroscopic effects over the course of a longer session were then analysed by checking peak accelerations and assessing the subjective feedback from the driver. Figure 72 shows how the acceleration levels are generally increasing, which contradict the expected result. When checking the actual scaling of forces, it could be verified that vulcanisation was indeed decreasing the available performance.

The normal case, framed in blue, was run earlier than the purple case, implying that the performance increment over the course of the session was higher with less experience. Upon further analysis it was found that the driver was simply improving the quality of the braking input, resulting in being closer to the optimal slip ratio. He was therefore able to achieve higher accelerations and move the braking point on average 4 m later per 10 laps during the first session.

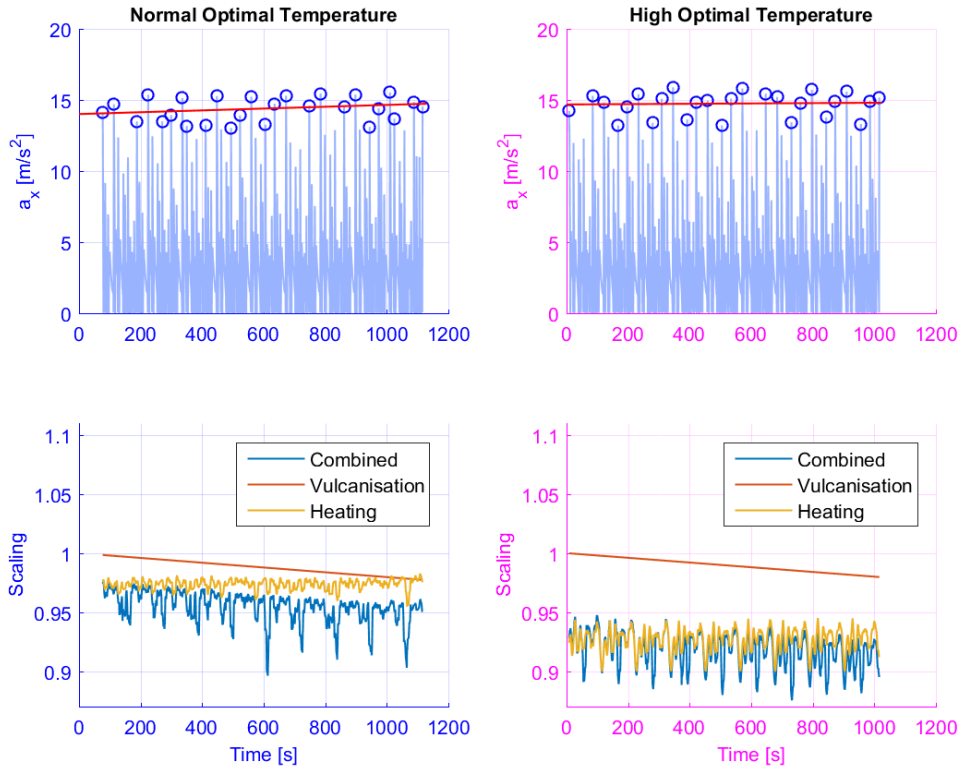

Figure 72 – Higher longitudinal accelerations despite lower grip

The driver considered this longitudinal performance to be realistic in that the change was barely noticable, while noting that this may vary between tracks and that its correlation to temperature fluctuations was of greater importance than the slow vulcanisation phenomena.

5.2.3 Cornering Stiffness

The transistion between cornering stiffness and lateral grip is determined by two transition points, as covered in Section 4.4. It proved crucial to ensure that the peak transition point P_{peak} was below the maximum recorded rear slip angle, shown in Figure 73, to ensure that scaling of stiffness wouldn't affect mid-corner car balance.

The reversible change of stiffness was rendered unreliable by the lack of stability in simulated inflation pressure and was therefore discarded. However, the increased stiffness from abrasion wasn't noticable thorugh the front axle as it tend to quickly leave the linear region, but ended up causing understeer on corner entry due to the lower slip angles on the rear axle. This phenomena exist in the real car, but is thought to arise more from a lack of grip on the front axle rather than higher rear stiffness, as it would persist in later stages of the corner.

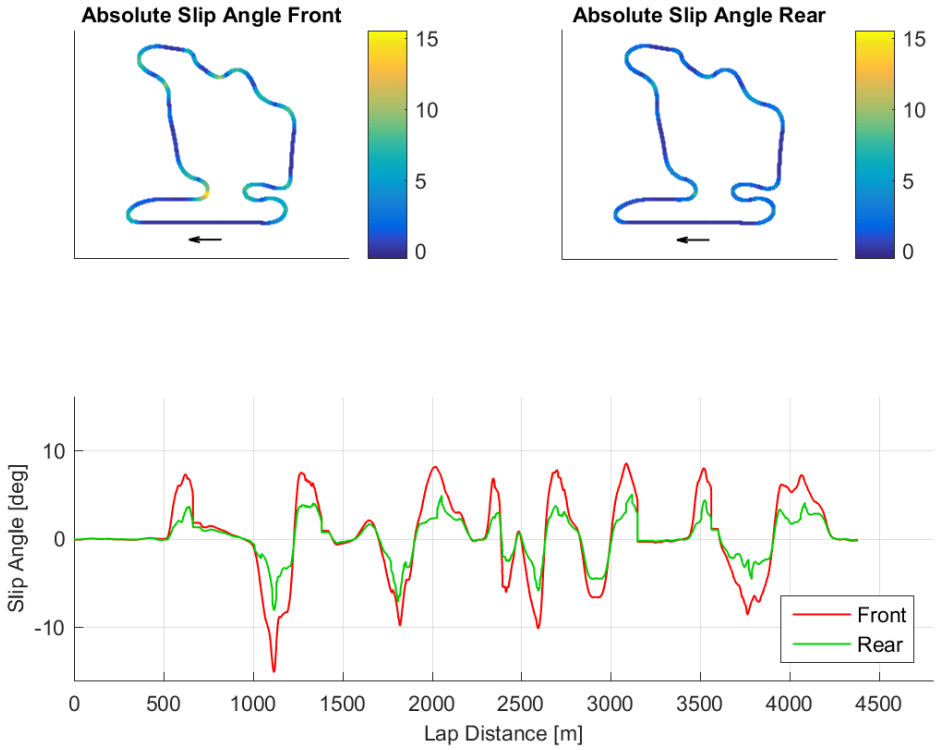

Figure 73 – Average slip angle for each axle

The amount of penalty applied when leaving the optimal temperature point was understood as primarily affecting stability during corner entry. The rear tyres would typically be closer to the optimal point as the front tyres overheat, resulting in that the driver would express concerns about poor *chassis responsiveness*, probably referring to the lower initial yaw responsiveness of the car. Once desired entry and mid-corner behaviour was reached, tuning the amount of heating penalty helped control the effects of excessive wheel slip on corner exit.

5.2.4 Lateral Grip

Reversible lateral grip scaling from the heating model is equal to its longitudinal counterpart. The effect was therefore crucial for overall vehicle balance, with the front tyres being significantly hotter throughout the corner and therefore sensitive to any applied penalty. Once realistic interplay between entry stability, mid-corner balance and propulsion behaviour was reached, the overall lateral grip loss over the course of a session could be evaluated.

Contrary to the longitudinal case, it can be seen in Figure 74 that peak accelerations were lower towards the end, which match the behaviour of the real car. The lower lateral grip cause the slower cornering speeds, which contributes to increased laptimes.

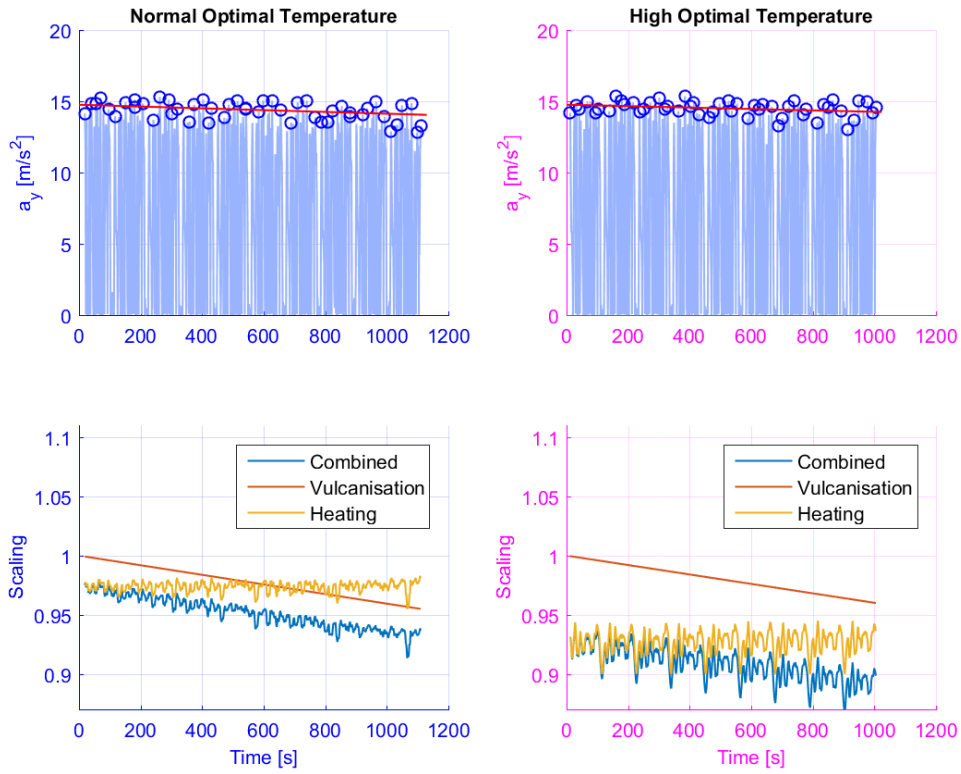

Figure 74 – Lateral accelerations and scaling of grip

While studying data from the car as it was driven without disturbance from opponents, it could be seen that a realistic target was for the laptime to increase by between 0.1 and 0.2 seconds per lap. This macroscopic affect was controlled by the vulcanisation penalty and the laptimes from a longer session in the simulator can be seen in Table 6.

Table 6 – Laptimes from a simulator session

	Hungaroring
Lap 1	1:51:261
Lap 2	1:51:509
Lap 3	1:51:849
Lap 4	1:51:697
Lap 5	1:52:766
Lap 6	1:52:412
Lap 7	1:53:169
Lap 8	1:52:406
Average Increment	**0.16 s / lap**

The driver was satisfied with the rate of performance loss, but also its effect on car balance. Due to the front tyres being the ones that experience highest forces during both braking and propulsion, but also the highest slip angles, it is natural for them to loose more grip than the rear tyres. The real car would therefore run with a mechanical setup so that it has tendencies of oversteer during the early parts of the race. The car will then be neutral during the middle portion of the session, as the front tyre grip fade away.

These trends were apparent when the evolution model was used in the simulator, allowing the driver to judge performance over a wider balance span.

6 Discussion

During the first part of the thesis, several reports covering the topic of tyre degradation were studied. As expected, their primary focus was on road car tyres and mostly wear in the form of rubber abrasion. Its influence on actual tyre performance was rarely covered, so finding alternative ways of understanding the mechanics behind grip loss has proven important.

Experienced motorsport engineers will use phrases such as *"running the tyres too hot"* or *"being outside the temperature window"* to describe tyre operation. This implies that the thermal state of the tyre is of greater importance that just the type of mechanical stress that it is being subjected to. Abrasive wear exist as a phenomena within motorsport, but using it as a measure of tyre life is not sufficient.

After a session, rubber which have been worn off will typically roll up and get stuck to the hot surface, as seen in the left part of Figure 75. The right part shows how the surface looks after having gone through the process of *scraping*. This is done by heating the surface with a heat gun and then removing worn rubber using a steel scraper. This allows for better contact with the road surface, in case the tyre is to be used again. The amount of rubber abrasion is typically so small that some segments still have the moulding patterns from manufacturing left, as seen in the upper right part of the picture.

Figure 75 – Partially scraped tyre

6.1 Resources

Other documented approaches to tyre degradation were primarily focued on slip power, rendering them unable to capture the accumulated damage that comes with bringing the temperature up to high levels. In order to capture loss of performance, it was therefore important to focus on the thermal aspects of tyre performance. This required a large portion of the development time to be spent on modelling temperature fluctuations.

The decision to split the simulated tyre in multiple lateral segments with uneven loading added further complexity, but enabled the model to better reflect setup changes, primarily in terms of camber.

The latter part could have been discarded for basic use in terms of driver training rather than car development, allowing greater focus on modelling the rim as a thermodynamic element and further tuning of scaling factors.

The driving simulator offers good immersion and has been thoroughly used to prepare drivers and engineers ahead of race weekends. It was therefore a great tool for the subjective assessment of this thesis.

The available data has been extensive, particularily from the cars. The only addition which could have aided the project would be to measure temperature of both inside and outside of the rims. The tyres were tested in dedicated rigs prior to the start of the project. There was data from various pressure levels, but also from tyres at different points on their life cycle. Here, the only valuable addition would have been to run the test on hotter tarmac. As seen in Figure 76, most tyre measurements were carried out at road temperatures between 10 to 15 ℃, with no readings above 25 ℃. This is not representative of the race tracks that are visited around the world, but still offered valuable data.

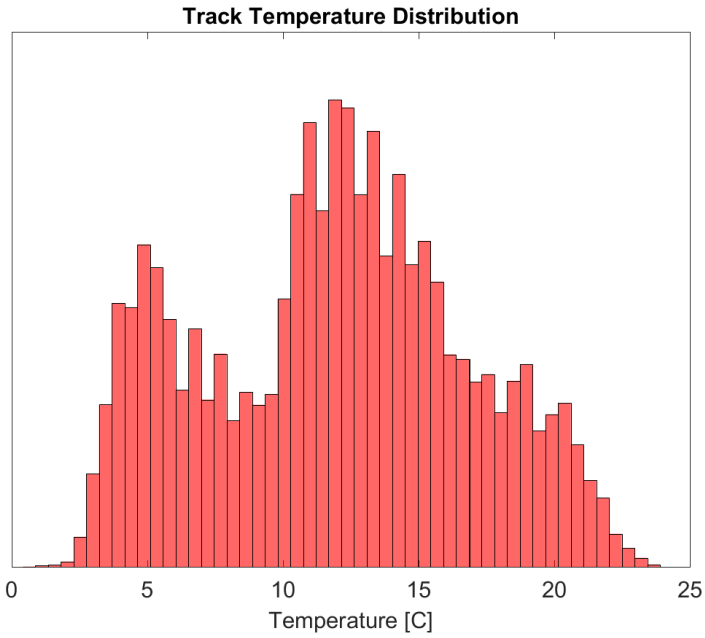

Figure 76 – Track temperature distribution from tyre tests

6.2 Conclusions

When evaluating performance of a race car on the track, the biggest issue is often that the tyres are changing. This makes it difficult for drivers to compare changes in roll stiffness, kinematics and wheel alignment. It can therefore be argued that being able to simulate the evolution of tyre performance is somewhat defeating the purpose of using a driving simulator. However, if the mechanics behind loss of tyre performance are understood, this model can help the engineers fast forward to various stages of the race and let the driver judge how a certain setup respond in those conditions. The change of performance can also happen in discrete steps rather that the continuous nature of the real world, allowing for a more clear comparison.

The model which enabled this type of testing was developed so that its parameters could be identified by analysing logged vehicle data. This, in combination with its modular structure allowed for easy control and setup. It also enables adding features such as oscillations from debris or disabling irreversible performance loss.

In terms of parameter tuning, it was surprising how small effect cornering stiffness had on the perceived agility of the front axle. While logical, its effect on rear axle stability was equally unexpected. It prevented the car from initialising its rotation when approaching a corner and therefore ended up compromising the remainder of the turn.

The vulcanisation model worked well and offered desired performance loss. The driver was pointing out that unless aggressive driving and overheating of the tyre is penalised, the usefulness of the model would be significantly reduced.

By defining the optimal temperature as a point rather than a range, its sensitivity to fluctuations increased. This is probably unnecessary and it made the model more difficult to tune, so either defing a range or using the shape of a polynomial rather than the current solution is likely to be better. It should also be noted that deviating a certain amount may cause a different amount of performance loss depending on whether it's above or below the optimal point.

The load distribution model was known to exaggerate pressure migration upon high vertical force or large camber angle. This occurs primarily on the outer front tyre upon braking into a turn, possibly affecting the heat generation and thereby deviation from optimal temperature.

Targeting usage in a driving simulator has proven to be a good exercise in creating robust solutions. The inputs of the driver are unpredictable, offering several challenges that must be considered.

6.3 Recommendations

The abrasive wear probably has an insignificant effect on tyre stiffness in a motorsport application. However, it may be so that a thinner sheet of rubber offer less material for hysteretic energy dissipation, making it more difficult to keep the tyres up to temperature, but also potentially lower the overall grip.

Splitting the tyre in multiple lateral segment allow for greater understanding of how to utilise the full width of the contact patch. However, rather than connecting inflation pressure to cornering stiffness, more value can probably come from understanding how it influences load distribution over the contact patch. Side wall failure due to overload is not uncommon since teams run with large camber angles to maximise cornering performance. Carrying out measurements of spring compression and camber on the real car could provide a foundation for correlating temperature build-up over the width of the tyre to vertical loading and wheel alignment.

It could also be beneficial to pay more attention to the heat transfer that takes place outside of the contact patch. As seen in Figure 77, the rubber will be cooled down during a short period as it's pressed against the road. The rubber block then starts to slide, generating heat which is to be cooled as it then travels through the air over the remainder of the rotation.

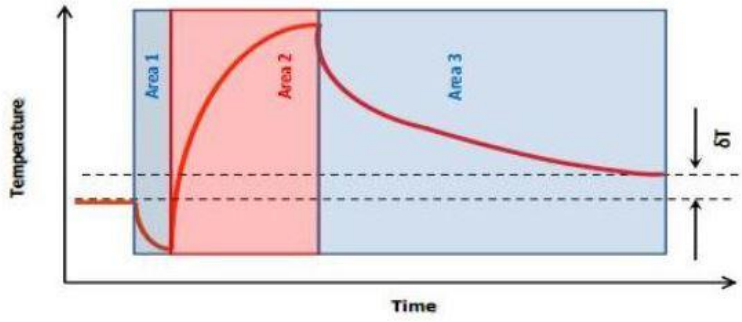

Figure 77 – Tyre heat transfer (Haines, 2011)

The surface temperature will play a role in determining the core rubber temperature. However, the gradient between outer and inner surface may have a significant effect in rate of vulcanisation. It may also be influenced by the level of mechanical stress that is being applied to the rubber.

As for all effects, the track surface will play a significant role. Rough road texture may favour the hysteresis component of grip while a flatter surface relies on good adhesion. Understanding how the frequency content of a given road texture will affect grip would add great value to the model.

List of References

Catsburg, N. (2017). WTCC Driver - Simulator sessions and interviews.

Cyan. (2016). Cyan Racing - Logdata from tests and races.

Dunlop. (2010). *F1 - Motorsports - Tyre graining explained*. Retrieved from Youtube - NextgenAutoVideos: https://www.youtube.com/watch?v=y9jC6sUOkR4

Farroni, F., Russo, M., Riccardo, R., & Timpone, F. (2014). A physical-analytical model for a real-time local grip estimation of tyre rubber in sliding contact with road asperities. *Journal of Automobile Engineering*.

Gent, A. N. (2007). Mechanical properties of rubber. *Tire mechanics short course.*

Guiggiani, M. (2014). *The Science of Vehicle Dynamics.*

Haines, D. (2011). *Tyre Temperature Measurement for Improved Tyre Modelling.* Cranfield University.

Haney, P. (2003). *The Racing & High-Performance Tire.*

Knisley, S. (2002). A correlation between rolling tire contact friction energy and indoor tread wear. *Tire Science and Technology 30*, 83 - 89.

Lupker, H., Cheli, F., & Braghin, F. (2004). Numerical prediction of car tire wear. *Tire Science and Technology 32*, 164 - 186.

MathWorks. (R2015b). *MATLAB & Simulink*. Retrieved from https://mathworks.com/

Menneglier, M. (2017). Conversation. (H. Richardson, Interviewer)

Michelin. (2001). *The tyre grip.* Société de Technologie Michelin.

Milliken, W., & Milliken, D. (1995). *Race Car Vehicle Dynamics.*

Mohlin, M. (2017). Discussions about race tyres. (H. Richardson, Interviewer)

Pacejka, H. B. (1992). *The Magic Formula Tyre Model.*

Persson, B. N. (2014). *Role of Frictional Heating in Rubber Friction.*

Persson, B., Tartaglino, U., Albohr, O., & Tosatti, E. (2005). *Rubber friction on wet and dry road surfaces.*

Pirelli. (2011). *Tyre Temperatures and Blistering*. Retrieved from Motorsport Week - Youtube: https://www.youtube.com/watch?v=2BNTFyxUhu0

RD. (2017). *Tire construction*. Retrieved from Rimsdealer: http://www.rimsdealer.com

Santos, R. (2014). *The absolute guide to racing tyres*. Retrieved from Racing Car Dynamics: http://racingcardynamics.com/

Tyrecity. (2017). *Tyre pressure*. Retrieved from Tyrecity: http://www.tyrecity.co.uk

Veen, J. (2007). *An analytical approach to dynamic irregular tyre wear.*

Wright, C. (2017). *The Contact Patch*. Retrieved from http://the-contact-patch.com/

Appendix A : Model Overview

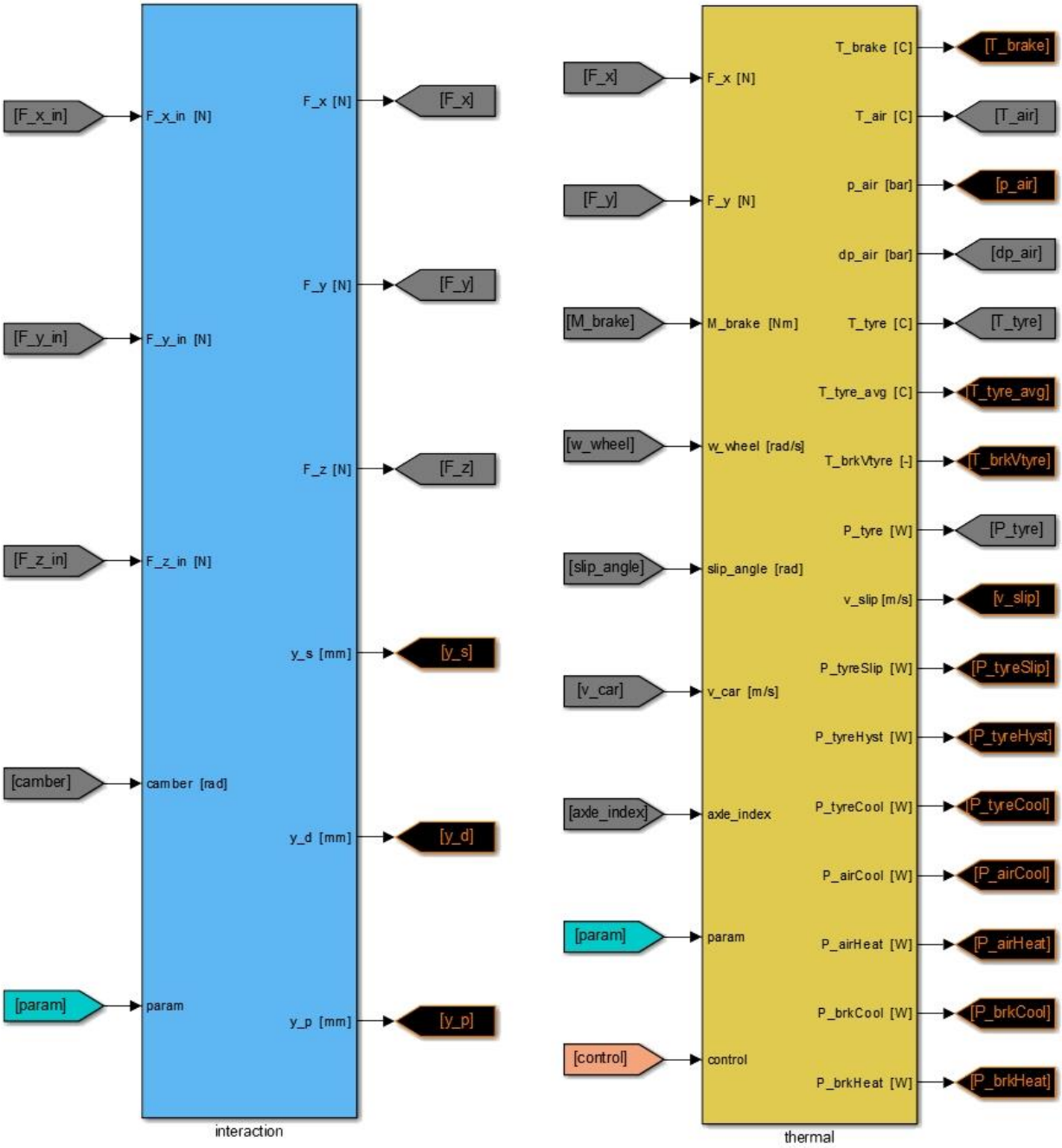

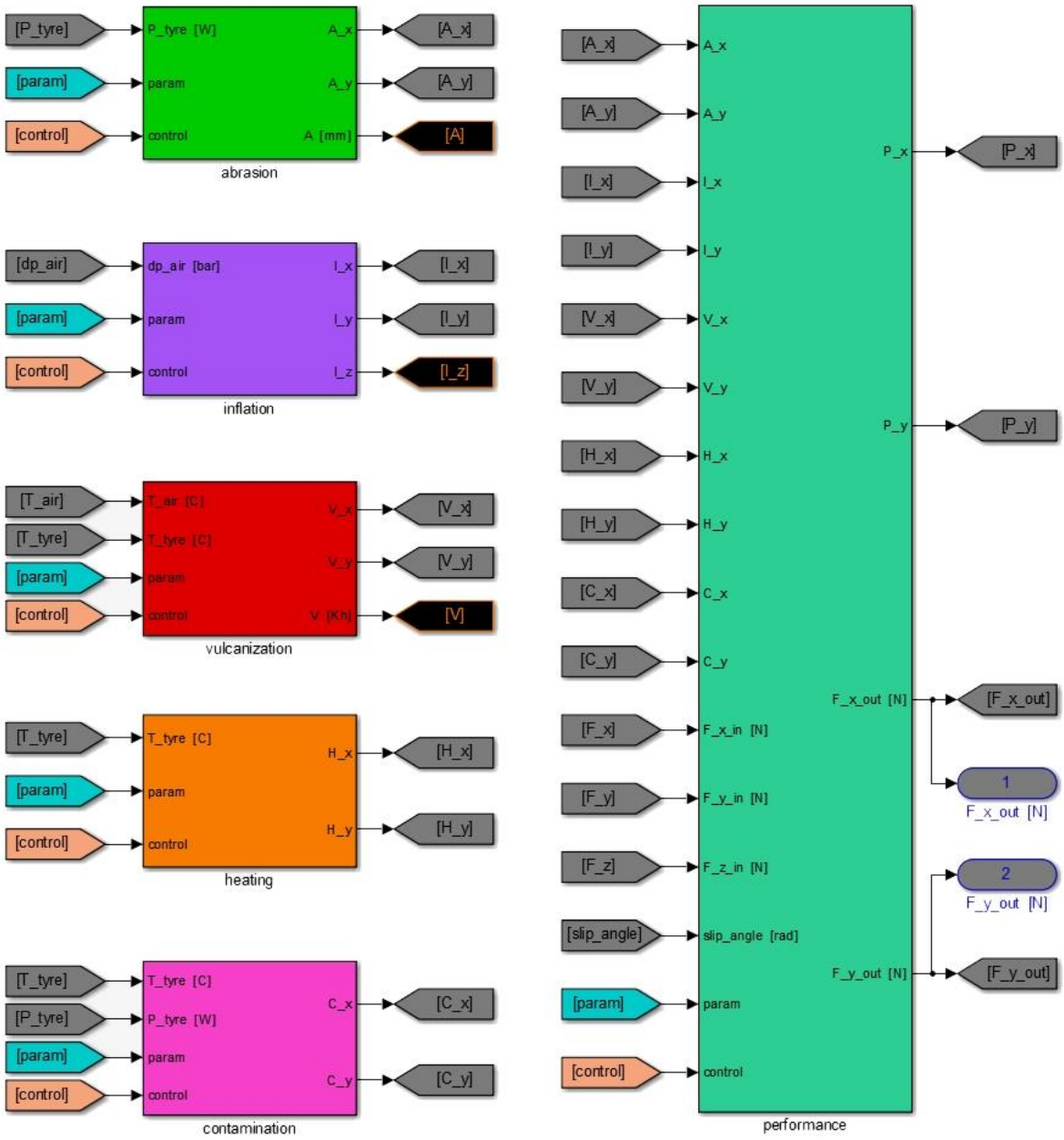
[P_tyre]
[param]
[control]
P_tyre [W]
param
control
A_x
A_y
A [mm]
[A_x]
[A_y]
[A]
abrasion
[dp_air]
[param]
[control]
dp_air [bar]
param
control
I_x
I_y
I_z
[I_x]
[I_y]
[I_z]
inflation
[T_air]
[T_tyre]
[param]
[control]
T_air [C]
T_tyre [C]
param
control
V_x
V_y
V [Kh]
[V_x]
[V_y]
[V]
vulcanization
[T_tyre]
[param]
[control]
T_tyre [C]
param
control
H_x
H_y
[H_x]
[H_y]
heating
[T_tyre]
[P_tyre]
[param]
[control]
T_tyre [C]
P_tyre [W]
param
control
C_x
C_y
[C_x]
[C_y]
contamination
[A_x]
[A_y]
[I_x]
[I_y]
[V_x]
[V_y]
[H_x]
[H_y]
[C_x]
[C_y]
[F_x]
[F_y]
[F_z]
[slip_angle]
[param]
[control]
A_x
A_y
I_x
I_y
V_x
V_y
H_x
H_y
C_x
C_y
F_x_in [N]
F_y_in [N]
F_z_in [N]
slip_angle [rad]
param
control
P_x
P_y
F_x_out [N]
F_y_out [N]
[P_x]
[P_y]
[F_x_out]
1
F_x_out [N]
2
F_y_out [N]
[F_y_out]
performance

Appendix B : Force Estimation Code

```
%% Input
a_x       : Longitudinal acceleration [m/s^2]
a_y       : Lateral acceleration [m/s^2]
wdot_z    : Yaw acceleration [rad/s^2]
v_x       : Vehicle Speed [m/s]

%% Vehicle data
h_CoG     : Centre of gravity height [m]
n_wbF     : Weight fraction fraction for front axle
n_rsF     : Roll stiffness fraction for front axle
h_rcF     : Roll centre height front [m]
h_rcR     : Roll centre height rear [m]
m_car     : Weight of car [kg]
cdA       : Drag coefficient times frontal area
clfA      : Front axle lift coefficient times frontal area
clrA      : Rear axle lift coefficient times frontal area
w         : Track width [m]
L         : Wheel base [m]
R         : Wheel radius [m]
I_car     : Yaw inertia [kg/m^2]

%% Air density and gravitational acceleration
rau = 1.2;
g = 9.81;

%% Normal Loads
% CoG lever arm to roll axis
dh = h_CoG - (n_wbF * h_rcF) + ((1 - n_wbF) * h_rcR);

% Load split in longitudinal, static, aerodynamic, elastic & geometric
F_z_long = (m_car * a_x / 2 * h_CoG / L) .* [-1; -1; 1; 1];

F_z_static = (m_car * g / 2) .* [n_wbF; n_wbF; 1-n_wbF; 1-n_wbF];

F_z_aero = - (rau / 2 * v_x^2 / 2) .* [clfA; clfA; clrA; clrA];

F_z_elast = (m_car * a_y * dh / w) .* [-n_rsF; n_rsF; n_rsF-1; 1-n_rsF];

F_z_geom = (m_car * a_y / w) .* ...
           [h_rcF; h_rcF; h_rcR; h_rcR] .* ...
           [-n_wbF; n_wbF; n_wbF-1; 1-n_wbF];

F_z = F_z_static + F_z_elast + F_z_geom + F_z_long + F_z_aero;

F_z(F_z <= 0) = 0;
```

```
%% Road Plane Force Assumptions
% Sum of lateral forces are equal to lateral acceleration times mass
% Lateral difference between axles give rise to yaw acceleration,
% neglecting the potential contribution from longitudinal forces.
FyR = - ((I_car * wdot_z) - (m_car * a_y * L) * (1 - n_wbF)) / L;
FyF = m_car * a_y - FyR;

% Find vertical forces for each axle
FzF = sum(F_z(1:2));
FzR = sum(F_z(3:4));
FzT = sum(F_z);

% Drag induced longitudinal force
FxD = (cdA * rau) / 2 * v_x^2;

% Front axle provides propulsion, brake distribution is assumed ideal
if a_x > 0
    FxF = m_car * a_x + FxD;
    FxR = 0;
    M_brk = zeros(4,1);
else
    FxF = (FzF/FzT) * (m_car * a_x + FxD);
    FxR = (FzR/FzT) * (m_car * a_x + FxD);
end

% Assume constant friction and distribute road-plane forces accordingly
F_y = [F_z(1:2) ./ FzF .* FyF; ...
       F_z(3:4) ./ FzR .* FyR];

F_x = [F_z(1:2) ./ FzF .* FxF; ...
       F_z(3:4) ./ FzR .* FxR];

F_z(F_z == 0) = NaN;

% Assume that brake torque is propotional to longitudinal braking force
if F_x(1) < 0
    T_brk = F_x * R;
else
    T_brk = zeros(4,1);
end
```

Appendix C : Simulator Session Test Plan

Session fundamentals

Exercise	Timed laps	Time Estimate
1. Tyre curve vs slip angle, turn-in to apex regions 2. Stiffness and peak fundamentals 3. Reversible vs irreversible		20 min

New tyre calibration [Hungaroring]

Exercise	Timed laps	Time Estimate	
• Check balance of car and find good baseline • Target qualifying peak performance • Run with **Page 1** to avoid confusion	2 + 2	11 min	

	lmux	lmuy
Front	1.112	1.01
Rear	0.98	0.9

Function test [Hungaroring]

Exercise	Timed laps	Time Estimate	

• Start with guidance in cockpit
  ○ Model DISABLE, PAUSE, ENABLE, RESET
  ○ Variables NEXT, PREVIOUS, UP, DOWN, RESET
  ○ Display 1, 2, 3, 4 (won't affect dynamics)
• Get familiar with driver controls
• Examples
  ○ ENABLE model
  ○ Lower heating penalty H_{xy}
  ○ Higher vulcanization penalty V_{lat}
  ○ BOX and PAUSE on pit entry
  ○ **Variable Reset**
• Stay in car, keep session running
	2	7 min	

Model shakedown [Hungaroring]

Exercise	Timed laps	Time Estimate	
• ENABLE model on pit exit • Feedback over radio whenever it arises	5	15 min	

Corner entry tuning [Hungaroring]

Exercise	Timed laps	Time Estimate	
• ENABLE model on pit exit • Wheel spin on out lap • PAUSE on main straight • Feedback over radio whenever it arises • Tune stiffness increase A_{cs} and inflation I_{cs} • Stop session	4	12 min	

Qualifying run [Hungaroring]

Exercise	Timed laps	Time Estimate	
• Model ENABLED on out lap and PAUSE on main straight • Find benchmark pace for new tyres • BOX and PAUSE on pit entry • Stay in car, keep session running	5	15 min	

Accelerated vulcanization run [Hungaroring]

Exercise	Timed laps	Time Estimate	
• Increase vulcanization penalty V_{lat} to remove grip • OPTION 4 • ENABLE model on pit exit • PAUSE on main straight • Target 1 second off benchmark pace	8	20 min	

Continue with longer race runs [Hungaroring, Shanghai..]